UNIVERSITÉ DE MONTRÉAL

DÉPARTEMENT DE BIOCHIMIE ET MÉDECINE MOLÉCULAIRE

FACULTÉ DE MÉDECINE

"The small subunit of the mitoribosome from *Andalucia godoyi*. Isolation and study of its protein composition"

Présenté par

José Angel Gonzalez Alcazar

Mémoire présenté à la Faculté de médecine

en vue de l'obtention du grade de maîtrise

en biochimie

20 mars 2018

UNIVERSITÉ DE MONTRÉAL

DÉPARTEMENT DE BIOCHIMIE ET MÉDECINE MOLÉCULAIRE

FACULTÉ DE MÉDECINE

Ce mémoire intitulé:

"The small subunit of the mitoribosome from *Andalucia godoyi*. Isolation and study of its protein composition"

Présenté par :

José Angel Gonzalez Alcazar

a été évalué par un jury composé des personnes suivantes :

Dr. Sebastian Pechmann

Dre. Gertraud Burger

Dr. Martin Schmeing

TABLE OF CONTENTS

LIST OF FIGURES AND TABLES

LIST OF ABBREVIATIONS

rRNA: ribosomal RNA

tRNA: transfer RNA

mRNA: messenger RNA

bt-rRNA: bacterial ribosomal RNA

cyt-rRNA: cytosolic rRNA

mt-rRNA: mitochondrial ribosomal RNA

mt-tRNA: mitocondrial transfer RNA

mt-mRNA: mitocondrial Messenger RNA

A: adenine

IF: initiation factor

EF: elongation factor

RF: release factor

mtIF: mitochondrial initiation factor

mtEF: mitochondrial elongation factor

mtRF: mitochondrial release factor

SSU: small subunit

LSU: large subunit

bt-SSU : small subunit of the bacterial ribosome

bt-LSU : large subunit of the bacterial ribosome

cyt-SSU : small subunit of the cytosolic ribosome

cyt-LSU : large subunit of the cytosolic ribosome

mt-SSU: small subunit of the mitochondrial ribosome

mt-LSU: large subunit of the mitochondrial ribosome

bt-SSU-rRNA: rRNA of the small subunit of the bacterial ribosome

mt-SSU-rRNA: rRNA of the small subunit of the mitoribosome

cyt-SSU-rRNA: rRNA of the small subunit of the cytosolic ribosome

bt-LSU-rRNA: rRNA of the large subunit of the bacterial ribosome

mt-LSU-rRNA: rRNA of the large subunit of the mitoribosome

cyt-LSU-rRNA: rRNA of the large subunit of the cytosolic ribosome

GDP: guanosine-5'-diphosphate

GTP: guanosine-5'-triphosphate

PTC: peptidyl transferase center

OPR: Open reading frame

5-prime UTR: 5-prime untranslated region

r-protein: ribosomal protein

mito-r-protein: mitoribosome protein

PPR : pentatricopeptide repeat

PES : polypeptide exit site

PAS : polypeptide accessible site

LECA: last eukaryotic common ancestor

mtDNA: mitochondrial DNA

BSA: bovine serum albumin

LC-MS/MS: liquid chromatography–mass spectrometry

ACKNOWLEDGMENTS

I want to thank Gertraud Burger for being my director and for the wonderful opportunity to work in her laboratory during my master's project. I also thank M. Valach for his support during the optimization of laboratory protocols and W. Gray for providing functional annotations of nucleus-encoded proteins.

Finally, I want to thank my family and God for being an unconditional support in my life.

RÉSUMÉ

Les mitochondries proviennent d'une alphaprotéobactérie ingérée qui a développé une relation endosymbiote permanente avec son hôte. Par la suite, la plupart des gènes de l'endosymbionte ont été perdus ou migrés vers l'hôte, et le mitoribosome a été remodelé en raccourcissant les ARNr mitochondriaux (ARNr-mt) et en recrutant de nouvelles protéines ribosomiques mitochondriales (protéines-r-mt). Pourtant, comment exactement ce remodelage évolutionnaire a eu lieu reste spéculatif en raison du petit nombre d'études chez les eucaryotes primitifs. Ici, nous montrons que la petite sous-unité du mitoribosome d'*Andalucia godoyi*, un jakobid hétérotrophe flagellé avec le génome mitochondrial le plus primitif, a une proportion élevée de composants de type bactérien par rapport à son homologue dans les eucaryotes hautement divergents. Nous avons trouvé dans l'analyse par spectrométrie de masse que la petite sous-unité du mitoribosome d'*A. godoyi* contient plus de protéines ribosomiques bactériennes (21 protéines) que son homologue dans tout autre eucaryote (9 à 20 protéines). Bien que la petite sous-unité du mitoribosome d'*A. godoyi* représente un stade plus primitif du remodelage des mitoribosomes, certaines des protéines spécifiques à la mitochondrie sont déjà présentes (S25, S29, S33, S35, Rsm22 et Mrp10), or dans une moindre mesure que dans la petite sous-unité du mitoribosome de *S. cerevisiae* (16 protéines) et *H. sapiens* (13 protéines). En outre, la petite sous-unité du mitoribosome d'*A. godoyi* ne contient pas les protéines-r-mt S22, S26, S27, S31, S34, S36, S37, S38, S39, S41, S42, S43, S44, S45, S46, S48, et S49 - dont la plupart sont spécifiques aux eucaryotes. Nos résultats, en combinaison avec les caractéristiques de type bactérien dans les ARNr-mt d'*A. godoyi*, démontrent que cet organisme possède la petite sous-unité du mitoribosome la plus primitive connue à cette date. La caractérisation des mitoribosomes primitifs peut constituer un point de départ pour l'étude des étapes précoces et intermédiaires de l'évolution du mitoribosome.

Mots-clés : *Andalucia godoyi*, mitoribosome, petite sous-unité, évolution, jakobids, Discoba, *Excavata*.

ABSTRACT

Mitochondria originated from an ingested *alpha*-proteobacterium that developed a permanent endosymbiont relation with its host. Thereafter, most of the endosymbiont's genes were lost or migrated to the host, and the mitoribosome was remodeled by shortening the mito-ribosomal RNAs (mt-rRNAs) and the recruitment of new mitochondrion-specific ribosomal proteins (mito-r-proteins). Yet, how exactly this evolutionary remodeling took place remains speculative due to the small number of studies in primitive eukaryotes. Here we show that the mt-SSU ribosome of *A. godoyi*, a free-living heterotrophic flagellated jakobid with the most primitive mitochondrial genome, has an elevated proportion of bacteria-like components compared to its counterpart in highly diverged eukaryotes. We found by mass spectrometry analysis that the mt-SSU ribosome of *A. godoyi* contains more homologs of bacterial r-proteins (21 proteins) than its counterpart in any other eukaryote (from 9 to 20 proteins). Although the mt-SSU ribosome of *A. godoyi* represents a more primitive stage of mitoribosome remodeling, some of the mitochondrion-specific proteins are already present (S25, S29, S33, S35, Rsm22, and Mrp10), yet to a smaller extent than in the mt-SSU ribosome of *S. cerevisiae* (16 proteins) and *H. sapiens* (13 proteins). Furthermore, the mt-SSU ribosome of *A. godoyi* lacks the mito-r-proteins S22, S26, S27, S31, S34, S36, S37, S38, S39, S41, S42, S43, S44, S45, S46, S48, and S49 -most of which are eukaryotic-specific. Our results, in addition to the bacteria-like features of *A. godoyi'*s mt-rRNAs, demonstrate that this organism possesses the most primitive mt-SSU ribosome known. The characterization of primitive mitoribosomes may be a starting point for studying the early and intermediate steps in mitoribosome evolution.

Key words: *Andalucia godoyi*, mitoribosome, small subunit, evolution, jakobids, Discoba, *Excavata*.

1. INTRODUCTION

1.1 Mitochondrial genomes

The mitochondrion is a double-membrane bounded organelle that is present in most known eukaryotic organisms. This organelle originated from an ingested *alpha*-proteobacteria and is an integrative part of extant eukaryotes. The mitochondrion provides cellular energy, and is involved in other cellular tasks such as signalling, cellular differentiation, cell death, maintaining control of the cell cycle, and cell growth (1).

Mitochondria contain their own genome that consists of several copies of a single circular chromosome. However, mitochondrial genomes have diverged to such a degree that makes difficult to recognize their bacterial origin. For instance, the number of genes in mitochondrial genomes is three orders of magnitude smaller than in typical bacterial genomes, and gene organization does not follow operon rules. Moreover, a single-subunit enzyme performs transcription in mitochondria instead of a four subunit RNA polymerase as in bacteria.

Mitochondrial evolution in different eukaryotic lineages have resulted in a great diversity of sizes, content, and organization of mtDNAs. For instance, mitochondrial DNA (mtDNA) can vary in length from 6 to 2,400 kb and be present in many thousands of copies depending on the specie or cell type. *Chromera velia* contains the smallest mitochondrial genome, which harbors only 2 protein-coding genes (2). The most gene-rich mtDNAs containing ~100 genes are found in a recently discovered eukaryotic group, the jakobids, which will be discussed in more detail in later sections.

Extant mitochondrial genomes have lost most of their ancestral bacterial genes due to (i) deletion of genes that are no longer needed for survival of the endosymbiont and (ii) unidirectional transfer of genes to the nucleus (3, 4). Gene migration from mitochondria to the nucleus has been explained by the mutagenic nature of reactive oxygen species that arise from the electron transport chains, population genetic aspects, and the physical polarity of endosymbiosis creating a one-way street of gene transfer from lysed organelles

to the nucleus (5-8). Moreover, DNA transfer from an organelle to the nucleus does not have sequence-specific barriers (4, 9-11).

The mitochondrial genomes of all eukaryotes are thought to have retained genes that encode components of the electron transport chain due to the need of co-location for redox regulation, and to avoid the mistargeting of hydrophobic membrane proteins to the endoplasmic reticulum (4, 12, 13). Additionally, mitochondrial genomes encode ribosomal RNAs (rRNAs) and transfer RNAs (tRNAs) needed for the translation of mitochondrion-synthesized messenger RNAs (mt-mRNAs) (4). The rest of the mitochondrial proteins that are not mitochondrion-encoded are synthetized in the cytoplasm and then imported into the organelle (14).

The unidirectional transfer of genes from the mitochondrial genome to the nucleus seems to confer adaptive advantages to the eukaryotic cell too. For instance, the nuclear genes encoding mitochondrial proteins can be recombined by sex. Further, the mitochondrial DNA has a higher mutation rate than the nuclear DNA due to the oxidative stress that accumulates in mitochondria. Therefore, mutation in genes encoding mitochondrial proteins is reduced if these genes are nucleus-encoded (4).

1.2 The most bacteria-like mtDNAs

The mtDNA of jakobids, an order of eukaryotes in the megagroup of Discoba, appear to have the most bacteria-like mt-DNAs currently known due to their high number of mitochondrion-encoded transcripts, gene organization, structure of mitochondrion-encoded rRNAs (mt-rRNAs), and bacteria-like regulatory elements of gene expression.

The jakobid mtDNAs contain gene clusters that are densely packed and their gene rearrangement is generally alike to the one of free-living *alpha*-proteobacteria (15).

The jakobid mtDNAs encode molecules not usually encoded in the mtDNA of most eukaryotes. For instance, a four-subunit RNA polymerase, the *SecY* complex, the 5S rRNA, and an structural RNA linked to the mitochondrial RNP complex (15, 16). Moreover, the

5S rRNA is likely integrated in the mitoribosomes of jakobids since it is expressed in these organelles (17).

The mt-rRNAs of nine jakobids strongly resemble to the typical models of *E. coli* 16S and 23S rRNAs. The universal core of mt-rRNAs shares a high degree of sequence identity between jakobids and its bacterial counterparts. Furthermore, the mitochondrion-encoded genes possess upstream Shine-Dalgarno-like motifs that match to the 3-prime-terminal pyrimidine-rich motif in the mt-rRNA of the small subunit of the mitoribosome (mt-SSU-rRNA) (15).

1.3 Prokaryotic translation

Translations is the process by which a ribosome reads the sequence of mRNAs to synthesize proteins (18).

Translation of genes in Prokaryotes has been widely investigated and described (19-25). Prokaryotic translation can be divided in four steps: initiation, elongation, termination, and recycling. Several interactions between tRNAs, mRNAs, rRNAs, and proteins occur in every translation step to ensure the synthesis of correct peptides at the right time. In initiation, the initiation factors IF1, IF2, and IF3 recruit the initiator fMet-tRNAfMet and the small 30S subunit (SSU) to an AUG start codon (characterized by an upstream Shine-Dalgarno sequence in the mRNA). Then, the AUG codon and the f-Met-tRNA are positioned to the P site of the ribosome, and the large 50S subunit (LSU) is stably associated before starting the elongation step. In elongation, the ribosome selects the cognate aminoacyl tRNAs specified by the mRNA sequence that is bound to the A site of the ribosome. Then, the tRNA cognate to the next mRNA codon is transported to the A site in complex with the elongation factor (Ef-Tu) and GTP, which is followed by peptide bond formation with the tRNA in the P site. Subsequently, the nascent polypeptide is transported to the P site, and the elongation factor G (EF-G) catalyzes the translocation of the two tRNAs and the mRNA by one codon. Thereafter, the tRNA in the P site is ejected through

the E site and the elongation step is repeated until the ribosome reaches a stop codon defined by UAA, UAG, or UGA. The release factors 1 and 2 (RF1 and RF2) recognize the stop codon and release the nascent polypeptide. Then, the dissociation of RF1 and RF2 is promoted by the release factor (RF3). Subsequently, EF-G and the recycling factor (RRF) help to dissociate the ribosome subunits and the remaining tRNA in the P site. Finally, the ribosome subunits can be recycled for another translation cycle.

1.4 Translation in mammalian mitochondria

Translation of genes in mammalian mitochondria has been widely investigated (26-32). The mammalian mitochondria encode 9 monocistronic and two dicistronic mt-mRNAs. The mt-mRNAs have a modified codon usage with the standard UGA stop codon recognized as tryptophan and the standard AGA and AGG arginine codons being instead used as stop codons. The folding and excising of mt-tRNA structures is carried out by the mitochondrial tRNase Z ELAC2 and the mitochondrial RNase P respectively. The mitochondrial poly(A) polymerase adds a poly(A) end of approximately 50 nt to maturate every light-strand protein-encoding mt-mRNA. The translation of mt-mRNAs proceeds in three steps: initiation, elongation, termination and recycling (figure 1).

1.3.1 Initiation and elongation in mammalian mitochondrial translation

The small subunit of the mitoribosome (mt-SSU ribosome) recruits the mt-mRNA that is bound to the initiation factor mtIF3 (figure 1). This step blocks the reassociation of the mt-SSU with the large subunit of the mitoribosome (mt-LSU ribosome) (33). The mitoribosome recognizes either of three initiation triplets AUG, AUA, and AUU. Then, the initiation factor mtIF2:GTP recruits the f-Met-tRNA to the initiation triplets (34). Subsequently, the mt-SSU forms a complex with the mt-LSU. This prompts the hydrolysis of mtIF2-bound to GTP producing GDP and liberating the initiation factors mtIF2/mtIF3 from the mt-SSU.

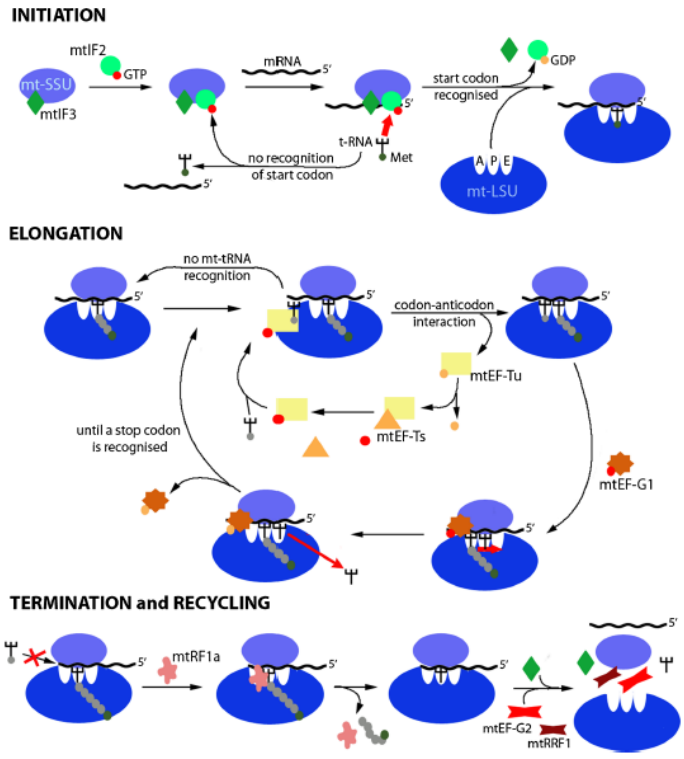

Figure 1. Translation on mammalian mitochondria proceeds in four consecutive steps: Initiation, elongation, termination, and recycling. The elongation factor mtEF-G1 interacts with the mitoribosome, which leads to changes in the structural conformation of the mitoribosome. This liberates the mitochondrial transfer RNA (mt-tRNA) from the A-site and moves the dipeptidyl-tRNA into the P-site. Then, the deacylated mt-tRNA moves to the E-site (35, 36). The elongation step is repeated until a stop codon is located in the A-site. Adapted from (33).

The elongation factor mtEF-Tu, a GTP and a charged mt-tRNA form the ternary complex (GTP:mtEF-Tu complex) that enters the A site (figure 1). Then, the mitoribosome hydrolyzes GTP to liberate GDP and mtEF-Tu. Subsequently, the peptidyl transferase centre (PTC) in the mt-LSU catalyzes the formation of the peptide bond. The dipeptidyl-tRNA moves to the P-site and a new deacylated mt-tRNA enters the A-site. The movement of the mt-tRNA and the mt-mRNA is guided by the mtEF-G factor during translocation

(37). Finally, the interaction between mtEF-Tu and the exchange factor mtEF-Ts re-establishes the GTP:mtEF-Tu complex.

1.3.2 Termination of mammalian mitochondrial translation and recycling of mitoribosomes

In humans, the mitochondrial release factor mtRF1 recognizes the stop codons in mitochondrial open reading frames (OPRs) (figure 1) (38). Then, the ester bond between the mt-tRNA and the final amino acid is hydrolyzed. Other mammalian species may have other additional mitochondrial release factors (39).

The mitochondrial release factors mtRRF1 and mtEF-G2 help the dissociation of the mt-SSU and the mt-LSU (figure 1). This releases the mt-mRNA and the deacylated mt-tRNA (40, 41). Finally, mtRRF1 and mtEF-G2 are released to reinitiate the translation cycle in mitochondria.

1.4 Differences of translation in bacteria, and mammalian and yeast mitochondria

During translation initiation in bacteria, base pairing occurs between the Shine-Dalgarno sequence in the 5-prime untranslated region (5-prime UTR) located upstream of the start codon of the mRNA and the 3-prime end in the rRNA of the SSU. However, mammalian mt-mRNAs lack the 5-prime UTR and all mt-mRNAs are devoid of the 5-prime cap structure (32, 42). Yeast mt-mRNAs usually contain the 5-prime UTRs that are targeted by transcript specific activators (32, 43, 44).

The mitochondrial factors that regulate translation initiation, elongation, termination, and recycling of mitoribosomes are nucleus-encoded and operate in concert with the mitoribosomes. Many of these factors have homologs in bacteria, but specialization occurred in response to the evolutionary changes in the mitochondrial

genetic code, mitoribosome structure, mitoribosome composition and nature of mitochondrion-encoded transcripts (42).

Initiation factors such as IF1, IF2, and IF3 determine the accuracy and effectiveness of translation in bacteria (32). Mammalian and yeast mitochondria have only two initiation factors compared to bacteria, mtIF2 (homolog of bacterial IF2) and mtIF3 (homolog of bacterial IF3) (45, 46). Although a mitochondrial homolog of IF1 is absent, mammalian IF2mt could provide structural compensation for the lack of IF1 (47, 48).

In bacteria, there is a high number of interactions between binding sites in r-proteins (L5, and L25), helices in rRNAs (h38, h76, h77, and h84), and the elbow region in tRNAs (49). Since every tRNA-binding site that is known from bacteria is present in the mammalian mitoribosome, one may think that elongation is the most conserved translational step. Yet, in contrast to bacterial tRNAs, mt-tRNAs in mammals attach to the LSU only by the acceptor stem due to the great diversity of elbow region shapes in the mt-tRNAs (32). In bacteria, EF-Tu delivers tRNA to the ribosome and participates in decoding, and translocation is catalyzed by the elongation factor EF-G (32, 50). Mammalian mitochondria have the same elongation factors as bacteria. However, mammalian mtEF-Tu and mtEF-Ts differ in structure from their bacterial homologs (51, 52). Moreover, bakers' yeast mitochondria are lacking mtEF-Ts (32, 53).

The bacterial EF performs recycling of ribosomes too, whereas the RRF1mt and mtEF-G2 (an homolog of bacterial EF-G) perform recycling of mitoribosomes in mammalian and yeast mitochondria (41). In addition, a third mitochondrial dissociation factor, mtIF3 was proposed to play a role in the recycling of mitoribosomes in yeast and mammals (32).

A final difference is that stop codons in bacteria are recognized by two termination factors, RF1 and RF2, while mammalian and yeast mitochondrial translation systems only possess RF1 (54-56).

1.5 Ribosome composition

Ribosomes across the tree of life have a large subunit (LSU) and a small subunit (SSU) composed of r-proteins and rRNAs. These subunits work together to translate mRNAs into a polypeptide chain. All ribosomes share a conserved core structure mainly composed of rRNA and r-proteins localized near the ribosome surface (16). The interface between the LSU and the SSU has three binding sites for the tRNAs, the A site, the P site and the E site (figure 2) (57). The A site is the access point for the aminoacyl tRNA in the ribosome (except for the first aminoacyl tRNA that enters through the P site during translation initiation). The P site is where the peptide bond is formed, and the E site (exit site) is where the uncharged tRNA is ejected after its amino acid was used to form a peptide bond in the nascent polypeptide chain. As described above, the mRNA binds to the SSU and moves through the ribosome one codon a time during the elongation of the nascent polypeptide chain.

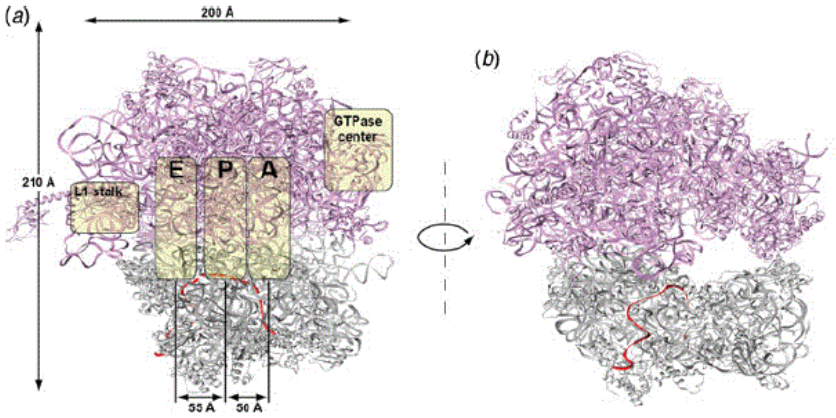

Figure 2. Structural view of the bacterial ribosome. (a) The 30S small subunit is displayed in gray and the 50S large subunit in purple, and the mRNA is displayed in red. The yellow covers indicate the localization of the L1 stalks, the tRNA-binding sites (A, P, and E sites), and the GTPase center. The tRNAs bind to the ribosome at the A site, passes through the P site, and exits through the E site. (b) The tunnel of the E site is observed occupied by the mRNA and the tRNA. Adapted from (25).

The different types of ribosomes differ in their RNA and protein content. For instance, eukaryotic (cytosolic) ribosomes have a rRNA: r-protein ratio that is close to one (50), whereas in bacterial ribosomes and in mammalian mitoribosomes, it is 7:3 and 3:7 respectively (33). The different types of ribosomes also differ in their sedimentation coefficient, length and number of rRNAs, and r-protein number (table 1).

1.6 The mammalian mitoribosome

The two subunits of bacterial ribosomes interact mainly via RNA:RNA bridges (58). In contrast, the intersubunit bridges of mammalian mitoribosomes are mainly composed by protein-protein and RNA-protein connections (35, 36). The 5S rRNA is absent from mammalian mitoribosomes and it is compensated by a tRNA-Val that forms several interactions with mitoribosome proteins (mito-r-proteins), which allows to mediate interactions between the mt-SSU and the mt-LSU (32, 49, 59, 60). The mito-r-proteins in the mammalian mt-LSU ribosome have contacts with an average of 4.9 neighbouring proteins whereas bacterial r-proteins have on average only 1.5 neighbors (49). Several mito-r-proteins, for instance S6, S16, S18, S25, L10, and L66, contain zinc-binding motifs that coordinate a single zinc ion between two proteins (16).

The mitoribosome recruited new proteins, and accumulated N- and C-terminal extensions of otherwise conserved proteins. In Mammalia, the mt-rRNA-was reduced, with mito-r-proteins replacing the missing rRNA segments, and providing additional functions such as association to the inner mitochondrial membrane (35, 36, 61).

Table 1. Summary of the composition in several characterized ribosomes.

	Eukaryotic cytosolic (62)	Bacteria (62)	Mammalian mitochondria (35, 36)	Yeast mitochondria (63, 64)	*Leishmania* mitochondria (63, 65)	*Trypanosoma* mitochondria (63, 66, 67)
Ribosome						
Sedimentation coefficient	80S	70S	55S	74S	50S	N/A
Number of rRNAs	4	3	3	2	2	2
Number of proteins	79-80	54	82	82	54	136
Large subunit						
Sedimentation coefficient	60S	50S	39S	54S	40S	40S
rRNAs	26S–28S (3,396–5,034 nt)	23S (2,904 nt)	16S (1,569 nt)	21S (3,296 nt)	12S (1,173 nt)	12S (1,150 nt)
	5.8S (156–158 nt)					
	5S (120–121 nt)	5S (120 nt)	CP tRNA (73–75 nt)			
Number of proteins	46-47	33	52	46	34	78
Small subunit						
Sedimentation coefficient	40S	20S	28S	37S	30S	25S
rRNAs	18S (1,800–1,870 nt)	16S (1,534 nt)	12S (962 nt)	15S (1,649 nt)	9S (610 nt)	9S (610 nt)
Number of proteins	33	21	30	36	20	58

Modified from (16). *; CP, central protuberance; N/A, not purified as a monosome.

The mt-mRNA entrance channel in the mt-SSU ribosome of mammals is highly remodeled regardless of the conservation of its central core (33, 61, 68). The mt-SSU ribosome of mammals lacks the protein S4 and the C-terminus of the protein S3, which are critical for defining the ringed shape of the mRNA entrance channel in the bacterial SSU

(bt-SSU) (figure 3) (33). This lost is compensated in mammalian mitoribosomes by extensions in the proteins S5 and S39 (a PPR-containing protein with RNA-binding activity) located close to the entrance channel (figure 3) (33, 69, 70). Moreover, the absence of the anti-Shine-Dalgarno motif and the 5-prime UTR in mt-mRNAs, which are needed to align the mitoribosome with the start codon, is compensated by the protein S29 (figure 3) (33, 71).

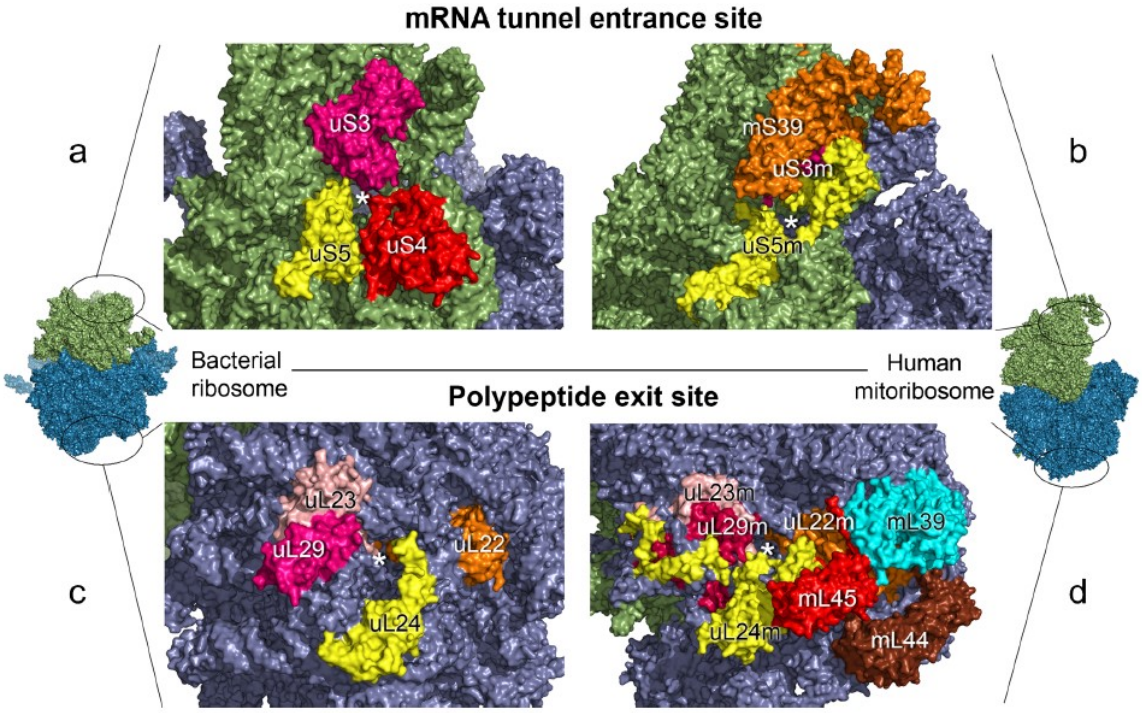

Figure 3. **Differences of mRNA entrance site and polypeptide exit site in bacterial ribosomes and human mitoribosomes**. The E. coli ribosome and the human mitoribosome are depicted left and right, respectively. The black circles in the monosomes indicate the expanded region for visualization purposes. The position of the mRNA entrance site in the small subunit of E. coli ribosome (a) and human mitoribosome (b) is shown at the top of the image. The position of the exit site in the large subunit of E. coli ribosome (c) and human mitoribosome (d) is shown at the bottom. Prefixes are used before or after protein names to indicate their nomenclature of origin: u + protein name refers to bacterial r-proteins, m + protein name to mito-r-proteins, u + protein name + m to proteins shared by both bacterial ribosomes and mitoribosomes. *; r-proteins, ribosomal proteins; mito-r-proteins, mitoribosome proteins. Adapted from (33).

The exit channel in the mammalian mt-LSU ribosome contains the mitochondrion-specific proteins L39, L44, and L45 that may play a role in the synthesis of hydrophobic proteins (33). Moreover, the mito-r-protein L45 is predicted to mediate the attachment of the mitoribosome to the inner mitochondrial membrane (42, 61).

1.7 The yeast mitoribosome

Overall, the secondary structure of the 15S mt-rRNA resembles that of the bacterial 16S rRNA with discrepancies only at the periphery of the mitoribosome (72). The 5S rRNA is absent in yeast mitoribosomes as described before in the human mitoribosome, which is compensated by mt-rRNA expansion segments rather than tRNAs as in mammals (32). The yeast mitoribosome possess most of the intersubunit bridges characteristic of bacterial ribosomes (72). Moreover, the mt-SSU ribosome of yeast possesses more homologs of bacterial r-proteins than its mammalian counterpart (72). The mt-mRNA entrance channel lacks the large-scale remodeling seen in the mammalian mt-mRNA entrance channel. Furthermore, the decoding center in the yeast mt-SSU ribosome is composed of a loop in the mito-r-protein S12 and several nucleotides that have equivalents in the decoding centre of bacterial ribosomes (72).

Although the yeast mitoribosome possess an elevated number of bacteria-like features compared to the mammalian mitoribosome, it also contains features that are unique to yeast. For instance, yeast specific mito-r-proteins and nine additional mitochondrion-specific intersubunit bridges. The majority of the yeast mito-r-proteins with homologs in bacterial and mammalian mitoribosomes have N- and C-terminal extensions that increase the protein interconnectivity, but these terminal extensions are not conserved in structure, sequence, or length across homolog mito-r-proteins (72). The 3-prime end sequence of the 15S mt-rRNA lacks the anti-Shine-Dalgarno sequences and is covered by proteins in the body of the mt-SSU ribosome in contrast to the bacterial 16S rRNA that possesses an anti-Shine-Dalgarno sequence and is restricted to the exit channel (72). Moreover, the yeast mt-mRNA exit channel is flanked by a protuberance in the S42-S43 heterodimer and extensions in several mito-r-proteins (72). Furthermore, Mba1 (homolog of mammalian

L45) and several mt-rRNA expansion segments attach the yeast mitoribosome to the inner mitochondrial membrane (42, 73, 74).

1.8 Mitoribosome composition in kinetoplastids

The kinetoplastids are a group of flagellate protists from the megagroup Discoba (to which jakobids belong) whose mitoribosomes have been extensively characterized. *T. brucei* contains 133 mito-r-proteins and *L. tarantolae* more than 50 mito-r-proteins (66, 75). The mitoribosome of kinetoplastids has few bacterial and mammalian homologs, and most of its constituent proteins are either kinetoplastid-specific or organism-specific (66, 75, 76). Moreover, most of the conserved mito-r-proteins are far lengthier than their homologs in bacteria, yeast, and mammals due to N- and C-terminal extensions (60, 66, 77-79).

The 9S and the 12S mt-rRNAs of *T. brucei* and *L. tarantolae* mitoribosomes are shorter and have a minimal secondary structure compared to their bacterial counterparts (75, 80). The additional protein mass in mitoribosomes of kinetoplastids, and lengthier N- and C-terminal extensions in homolog proteins may counterbalance the highly reduced nature of their mt-r-rRNAs (66, 80). The same phenomena has been observed, but to a lesser extent in mammalian mitoribosomes (59).

The mitoribosome of *T. brucei* contains a high number of unique mt-r-proteins (105 out of 136 mito-r-proteins) that could be part of a larger "supercomplex" associated with the mitoribosome that possess additional functions. For instance, some of these proteins contain PPR and GTP binding motifs. Moreover, some of these proteins possess predicted activities such as GTPase, methyltransferase, peptidyl-prolyl isomerase, helicase activity, and chaperone function. These motifs and functions potentially play a role in ribosome assembly, RNA folding, mt-rRNA processing, protein assembly, protein-RNA interactions, and subunit structure stabilization (66, 81).

In *L. tarantolae* mitoribosome, the mt-mRNA entrance and the exit channels contain *Leishmania*-specific mito-r-proteins. Moreover, these mito-r-proteins replace the missing rRNA segments in the A, P, and E sites (76).

1.9 Mitoribosome evolution

1.9.1 Evolution of the mitoribosome structure

Endosymbiotic bacteria tend to accumulate mutations that reduce the stability of their rRNAs and most mitochondrial genomes have a higher A+T content than bacterial genomes, which confers a higher number of weak base pairs to the mt-rRNAs (82). Moreover, high mutation rates, small effective population sizes, and low rate of recombination in mitochondria cause slightly deleterious mutations in the mt-RNAs (83).

Genome analysis of several model organisms showed that, compared to bacterial ribosomes, the protein mass of mitoribosomes is generally larger, while the length of most mt-rRNAs is similar or smaller. Although highly diverged eukaryotes have structurally reduced mt-rRNAs and an elevated number of mito-r-proteins, there is no strict correlation between the loss of mt-rRNA segments and the gain of mito-r-proteins (59).

It has been suggested that many mitoribosome proteins may have already been recruited early in eukaryotic evolution, converting the mitoribosome from “mt-rRNA rich and protein-poor” to “mt-rRNA rich and protein-rich” (figure 4) (59). The reduction of mt-rRNA may have started only when metazoan diverged and resulted in “mt-rRNA poor and protein-rich” mitoribosomes (figure 4).

Additionally, several N- and C-terminal extensions in mito-r-proteins occurred in different linages and separately, after the divergence of the last eukaryotic common ancestor (LECA), so that the length of homolog proteins can differ considerably.

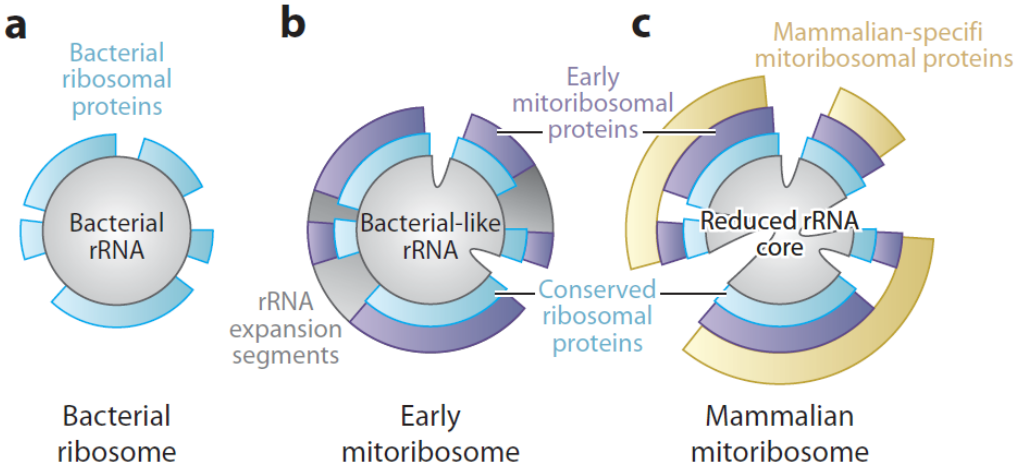

Figure 4. Representation of the constructive evolution of mitoribosomes. a) Proteobacterial ribosome, b) Early mitoribosome with additional rRNA expansion segments and early mitoribosome proteins. Adapted from (16).

1.9.2 Evolution of mitoribosome protein composition

The evolutionary history of mito-r-proteins has been traced in the phylogenetic tree of eukaryotes (figures 5 and 6) by the identification of homologs of *alpha*-proteobacterial r-proteins and mito-r-proteins in a wide range of nuclear, mitochondrial, bacterial and archaeal genomes (63). The phylogenetic tree based on mito-r-proteins indicates that 54 mito-r-proteins (21 in the SSU, and 33 in the LSU) were likely present in the *alpha*-proteobacterial ancestor of the mitoribosome (figure 6). The protein S20 was apparently lost early in eukaryotic evolution, since it is absent in all analyzed eukaryotic genomes (figure 6).

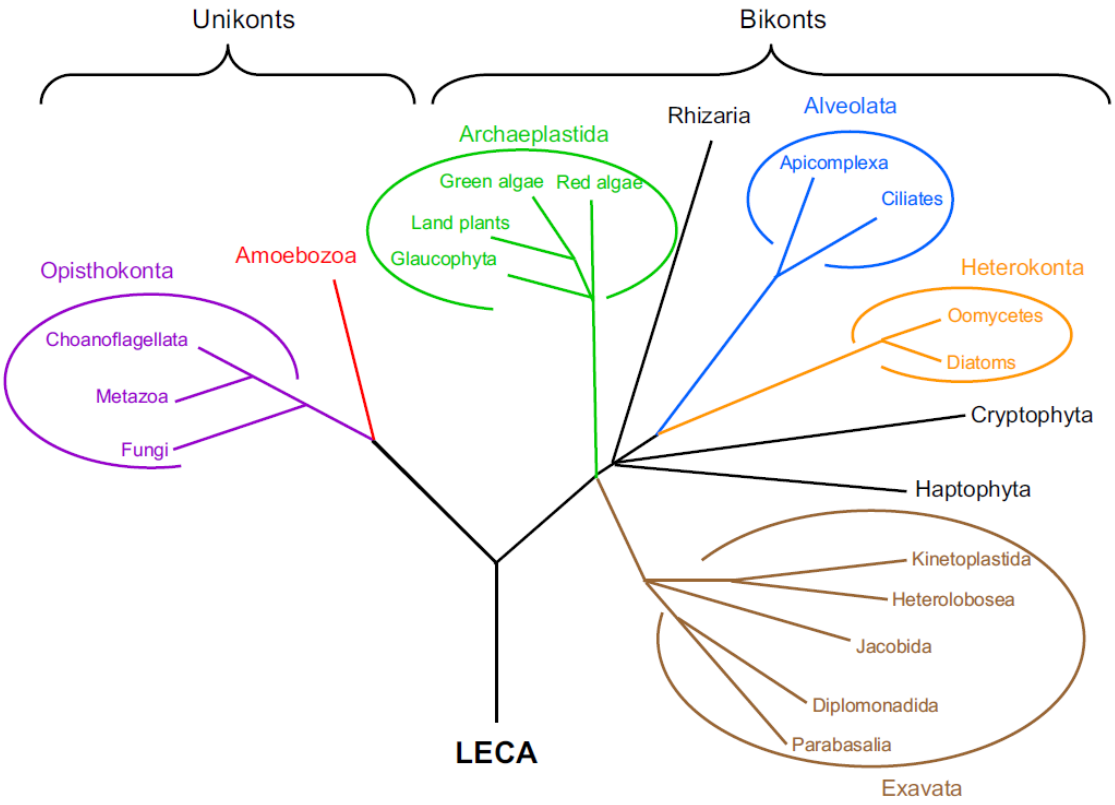

Figure 5. Phylogenetic tree of eukaryotes used to predict the evolutionary history of mitoribosome proteins. *; LECA, last common eukaryotic ancestor. Adapted from (63).

A set of 27 *alpha*-proteobacterial mito-r-proteins was likely encoded in the mitochondrial genome of the last eukaryotic common ancestor (LECA) because it is still encoded in the mitochondrial genome of *Reclinomonas americana* (84), a jakobid protist that contained the largest mitochondrion-encoded gene set that was known at the time of the analysis. The other 26 *alpha*-proteobacterial mito-r-proteins not encoded in any available mitochondrial genome were predicted to be relocated to the host nuclear genome before the divergence of the major eukaryotic linages (figure 6). The migration of genes encoding *alpha*-proteobacterial r-proteins from the mtDNA to the nucleus probably started before the recruitment of eukaryotic-specific mito-r-proteins since gene migration from endosymbionts to the host is a common event in endosymbiosis. Then, nineteen eukaryotic-specific mito-r-proteins were apparently recruited before the divergence of the LECA, which added up to a total of 72 mito-r-proteins (63).

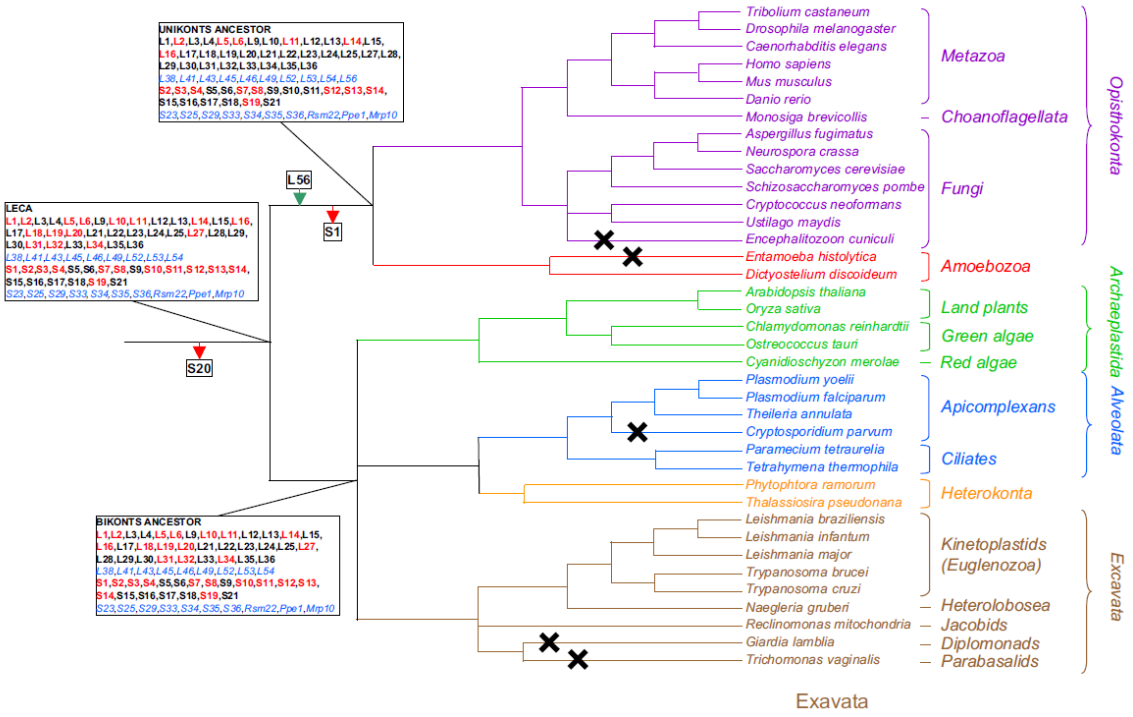

Figure 6. Prediction of mito-r-proteins possessed by the LECA and its following evolution in Bikonts and Unikonts. Red arrows designate losses of mito-r-proteins, whereas green arrows designate gains. The mitochondrion-encoded mito-r-proteins of *alpha*-proteobacterial origin are shown in bold. Mitochondrion-encoded mito-r-proteins are shown in red, whereas nucleus-encoded mito-r-proteins are shown in black. Eukaryotic-specific mito-r-proteins are shown in blue italic font. The crosses indicate eukaryotic linages that have lost their mitochondria. *; mito-r-proteins, mitoribosome proteins. Adapted from (63).

Considerable changes happened between the endosymbiosis and the diversification of present-day eukaryotic lineages because the LECA already possessed a remodeled mitoribosome and a quite developed genome reduction process after endosymbiosis (63). Losses and gains of mito-r-proteins are still ongoing as there are great differences between the mitoribosomes of closely related organisms (63). Gains and losses have occurred independently and repeatedly in different lineages. Moreover, there appears to be no general trend in protein dispensability since the losses have affected both *alpha*-proteobacterial and eukaryotic-specific mito-r-proteins (figure 6) (63).

1.10 *Andalucia godoyi*

The etymology of *Andalucia* refers to the region of Spain and it was named after José Godoy, a well-known philanthropist from Andújar, Spain (85). *Andalucia godoyi* is a member species of the jakobids.

Jakobids are small, bacterivorous, heterotrophic flagellates found in freshwater and marine habitats. They are unicellular eukaryotes typified by two flagella, one of which is guided posteriorly, and a devouring groove along the body utilized for uptake and ingestion of little particles and bacteria (86, 87). This group is a clade within Discoba and includes nine different genera: *Andalucia*, *Velundella*, *Stygiella*, *Moramonas*, *Jakoba*, *Stomatochone*, *Stenocodon*, *Reclinomonas*, and *Histiona* (85, 86, 88-92).

The two flagella of *A. godoyi* are inserted subapically and apically of its feeding groove (85) (figure 7). The cells have a size of 3–5 µl, and possess a paranuclear body and tubular mitochondrial cristae. The flagella are twice the length of the cell.

A. godoyi contains the largest mitochondrial gene set currently known (15). Moreover, its mtDNA encodes *trnT*, *cox15* and *rpL35* that are absent in the mtDNA of other jakobids.

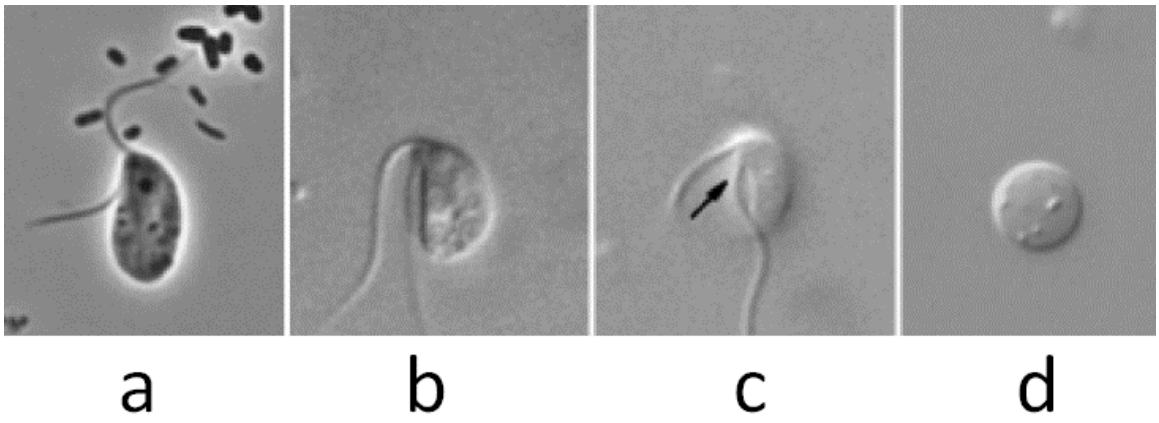

Figure 7. Light micrographs of *A. godoyi*. a) Static cell, b) Mobile cell, c) Mobile cell, an arrow points the feeding groove, d) Cyst. Adapted from (85).

2. HYPOTHESIS

In the course of eukaryotic evolution, the mitoribosome, has experienced losses of components originating from the ribosome of the bacterial ancestor and in turn has gained eukaryote-specific mito-r-proteins. Since the mitoribosome composition has been only investigated in highly diverged eukaryotes such as yeast, mammals, and kinetoplastids, the question arises when exactly and how this transition happened, gradually or as a wholesale restructuring. Since *A. godoyi* has the least diverged mitochondrial genome currently known, we expect that its mitoribosome represents an intermediate state in the transition from a bacteria-like ribosome to the mitoribosome as we know it from model organisms. **Therefore, we hypothesize that the *Andalucia* mitoribosome has a higher number of bacteria-like proteins and fewer mitochondrion-specific r-proteins than its counterparts in the model organisms discussed above.**

To test this hypothesis, we initially attempted to characterize entire mitoribosomes of this jakobid, but their purification proved extremely complicated. Therefore, we focused our investigation on the mt-SSU ribosome, which we succeeded to readily enrich. In fact, this subunit of the mitoribosome is more extensively remodeled than the mt-LSU ribosome, and thus is well suited for the study. Specifically, the objectives of this thesis are inferring the mitoribosome composition of *A. godoyi* from its genomic sequences, experimental characterization of its mt-SSU ribosome, and comparison with the composition in the mt-SSU of model organisms discussed above.

3. MATHERIALS AND METHODS

3.1 *A. godoyi* cell culture

A. Simpson kindly provided *Andalucia godoyi* (85). We feed *A. godoyi* using *Enterobacter aerogenes* as a food source. We grew *A. godoyi* in plastic culture bottles containing 15 ml

of WCL medium at 20 °C for 2 weeks. Subsequently, we transferred the culture to 100 ml of WCL medium and incubated it as specified before. Then, we transferred it to 500 ml of WCL medium and incubated it as specified before. The cells were checked regularly under the microscope and more *E. aerogenes* was added when most of it was consumed by *A. godoyi.* The titer at the stationary phase was $1.875x10^6$ cells/ml.

We harvested protist cells when all bacteria were consumed. The culture was centrifuged in a GSA rotor at 8,000 g for 20 min at 4 °C. The supernatant was discarded, and the pellet resuspended in 1 ml of WCL medium. Then, the cells were centrifuged at 7969 g for 3 min and the supernatant discarded. The cells were resuspended in 1% DMSO and stored at – 80 °C until their utilization.

3.2 Sucrose gradient purification of the small subunit of the mitoribosome (mt-SSU ribosome)

We tested four cell-lysis buffers with different ratios of monovalent to divalent ion concentrations (appendixes 8.2.9 to 8.2.16) (93). Then, we selected the buffer A because it produced the lowest degree of mt-rRNA degradation.

Andalucia cells were resuspended in one volume of homogenization buffer A and lysed with two volumes of lysis buffer A, 1X EDTA-free protease inhibitor, and SUPERase·In™ (4 U/µL) to inhibit the degradation of the mt-rRNAs. The homogenate was mixed and then incubated on ice for 5 min followed by centrifugation at 18,000 g for 10 min. The supernatant was loaded on top of a 5 ml 15-40 % sucrose gradient and centrifuged at 45,900 rpm for 3 h at 4°C using an AH-650 swinging-bucket rotor. Gradient fractions of 250 µL were collected using a micropipette from the top.

The mt-SSU ribosome of *A. godoyi* is present in the gradient fractions enriched in mt-SSU-rRNAs because intact ribosomes contain r-proteins bound to rRNAs. RNA was extracted from every sucrose gradient fraction to analyze the migration pattern of mt-rRNAs. We added 5 sample volumes of homemade trizol substitute and vortexed for 15 sec followed by 5 min of incubation at room temperature (94). Then, we added the

equivalent of one sample volume of chloroform and shacked vigorously for 30 sec followed by 5 min of incubation at room temperature. Subsequently, the samples were centrifuged at 20,000 g for 15 min at 4 °C and the upper aqueous phase was collected. 3 µl of glycogen (5 mg/ml) and 1.1 sample volumes of isopropanol were added followed by incubation for 40 min at 4 °C. Subsequently, the samples were centrifuged at 20,000 g for 15 min at 4 °C and the isopropanol was discarded. 200 µl of cold 70% ethanol were added and the sample centrifuged at 20,000 g for 10 min at 4 °C. Then, the 70% ethanol was discarded, and the RNA pellet was resuspended in 5 µl of DEPC-treated H_2O.

Every RNA sample was mixed with one sample volume of Thermo Scientific 2X RNA Loading Dye followed by incubation for 8 min at 80 °C and run at 110 mV in a 1 % agarose gel in 0.5x TBE. The run was stopped once the blue color of the loading dye was positioned 2.5 cm before the gel end. We used total RNA extracted from whole cells of *A. godoyi* as a positive control of mt-rRNA and cytoplasmic rRNA (cyt-rRNA), and total RNA extracted from *Enterobacter* as a control of contamination with bacterial rRNA.

We used the RNase-free DNase I from Roche® to digest the total RNA extracted from every sucrose gradient fraction. Briefly, 5 µl of total RNA were mixed with 5 µl of 1X reaction buffer, and 5 units of DNase I in a total volume of 50 µl followed by incubation at 37 °C for 30 min. Trizol RNA extraction was performed to remove the enzyme.

We utilized the avian myeloblastosis virus (AMV) reverse transcriptase from Roche to synthesize cDNA using rRNAs as a template. 0.8 µl of the above RNA sample were mixed with 0.5 µl of each 10 mM primer, and 1 mM of each dNTP followed by incubation at 80 °C for 2 min. Then, 1X of the reverse transcriptase buffer and one unit of the reverse transcriptase enzyme were added in a final volume of 10 µl followed by 1 h of incubation at 42 °C. Different primers were used to PCR-amplify each one of the ribosomal rRNAs in *A. godoyi* and *E. aerogenes* (table 2 and appendix 8.3).

Table 2. Primers used for RT of rRNAs (see the appendix 8.3).

Organism	Amplicon [a]	Ribosome type	Primer
A. godoyi	mt-SSU-rRNA	Mitoribosome	ag06
A. godoyi	mt-LSU-rRNA	Mitoribosome	ag02
E. aerogenes	16S bt-rRNA	Bacterial ribosome	ag06
E. aerogenes	23S bt-rRNA	Bacterial ribosome	ag02
A. godoyi	SSU-cyt-rRNA	Cytosolic ribosome	NS5

[a] mt, mitochondrial; bt, bacterial; cyt, cytosolic; rRNA, ribosomal RNA.

We used the Q5® High-Fidelity DNA Polymerase set from New England Biolabs and followed the guidelines of the supplier. Briefly, 0.25 µl of the cDNA were mixed with 0.2 mM of each dNTP, 0.5 mM of each primer, 1X Q5 buffer, and 0.05 µl of Q5 DNA Polymerase (2000 units/ ml). The annealing temperature was calculated with the Tm calculator v1.9.7 from the website of New England Biolabs [https://tmcalculator.neb.com/#!/main], as 2X (A or T) + 4X (C or G) -5 °C. We used different primer pairs and number of PCR cycles to amplify the cDNA synthesised from different rRNA types (table 3 and appendix 8.3). The thermal cycles were: 98 °C for 2 min, 98 °C for 10 sec, annealing temperature for 10 sec, 72 °C for 15 sec, go to step 2 (98 °C for 10 sec), 72 °C for 2 min, and 4 °C forever.

Table 3. Primers pairs and number of cycles used to amplify rRNAs.

Amplicon	Primer pairs [b]	Annealing temperature	PCR cycles
A. godoyi mt-LSU-rRNA	ag01 + ag02	63 °C	22
A. godoyi mt-SSU-rRNA	ag05 + ag06	68 °C	15
E. aerogenes 16S bt-rRNA	ag06 + eb04	68 °C	15
E. aerogenes 23S bt-rRNA	ag02 + eb01	66 °C	22
A. godoyi cyt-SSU-rRNA	NS5fwd + BMB-C-rev	70 °C	18

[a] mt, mitochondrial; bt, bacterial; cyt, cytosolic; rRNA, ribosomal RNA.

[b] for primer sequences, see Appendix 8.3.

3.3 Validation of the enrichment of the mt-SSU-rRNA

3.3.1 RNA quantification

We performed Northern Blot analysis of mt-rRNAs in order to quantify the enrichment of the mitoribosome subunits in sucrose gradient fractions. The RNA extracted from each sucrose gradient fraction was quantified in a NanoDrop machine before the electrophoretic separation of RNAs (table 4).

Table 4. RNA quantification of samples used in Northern blot.

Sample [a]	ng / µl	A260/A280 [b]	A260/A230 [c]
Enterobacter total RNA (R1)	1179	1.864	0.876
Andalucia total RNA (R2)	1118	1.816	0.683
Andalucia total RNA (R3)	1563	1.899	0.900
A	280	1.371	0.272
B	106	1.485	0.238
C	91.3	1.621	0.178
D	177	0.220	1.569
E	414	1.401	0.239
F	928	1.951	0.557
G	1021	1.315	0.275
H	270	1.737	0.289

[a] A, gradient fractions 1-2 (see figure 9); B, 3-4; C, 5-6; D, 7-8; E, 9-10; F, 11-12; G, 13-14; H, 15-16.

[b] A260/A280, Nucleic Acid 260/280 ratio calculated by dividing the absorbance of the sample at 260 nm between the absorbance at 280 nm.

[c] A260/A280, Nucleic Acid 280/260 ratio calculated by dividing the absorbance of the sample at 280 nm between the absorbance at 260 nm.

3.3.2 Electrophoretic separation of rRNAs

We conducted electrophoresis with the TT buffer (see appendix 8.2.18 for the composition) that was shown to improve the separation of long rRNAs (95). 4 µl of each RNA sample were mixed with 50% formamide, 1X of the TT buffer, 0.5 mM EDTA, and

0.02% bromophenol blue in a final volume of 8.5 µl followed by denaturation at 70 °C for 5 min. Subsequently, the samples were placed on ice and formaldehyde was added to a final concentration of 0.4 M. The samples were run at 6 V/cm in a 2 % agarose gel and a buffer containing 1.1% formamide and 1X TT buffer until the loading dye was positioned 2.5 cm before the gel end.

3.3.3 Radiolabelling of probes

We used the DNA probe ag03 for selectively highlighting the mt-SSU-rRNA, eb03 for 23S bt-rRNA, ag04 for mt-LSU-rRNA, and eb02 for bt-rRNA (table 5 and appendix 8.4). The oligonucleotides were radioactively labeled at their 5-prime end. For that, 2.5 µM of the oligonucleotide were mixed with 1X of the polynucleotide kinase (PNK) buffer, 2.5 of µCi/µl 6000 Ci/mmol [γ-^{32}P]-ATP, and 0.5 U/µl of the T4 PNK in a final volume of 20 µl followed by incubation for 45 min at 37 °C. Then, the enzyme was inactivated at 65 °C for 20 min. The unincorporated radioactive label was removed using NucAway™ Spin Columns according to the manufacturer's instructions.

3.3.4 Northern blot hybridization

The agarose gel was rinsed in DEPC-treated H_2O for 1 h and then soaked in 10X SSC transfer buffer. The nylon membrane was first saturated with milli-Q H_2O and then with 10X SSC buffer. We let RNA to transfer to the nylon membrane overnight in the Northern blot apparatus, and then we dried it at room temperature for a couple of min and marked the orientation of the membrane with a soft pencil. Subsequently, the membrane was dried for 2 h at 80 °C.

We qualitatively estimated the transfer efficiency by subtracting the RNA amount remaining in the agarose gel from the RNA amount that was loaded. The agarose gel was stained with 2.5 µl of ethidium bromide (10 mg/ml) while gently shaking for 15 min in 250

ml of 1X TT buffer. The picture was taken in a UV trans-illuminator to estimate the transfer efficiency.

Table 5. Probes used for Northern blot of rRNAs (see appendix 8.4).

Amplicon	Probe	Tm °C
mt-SSU-rRNA	ag03	59.7
mt-LSU-rRNA	ag04	61.4
16S bt-rRNA	eb02	62.5
23S bt-rRNA	eb03	64.4

*; mt, mitochondrial; bt, bacterial; rRNA, ribosomal RNA.

The nylon membrane was incubated with I) 2X SSC buffer for a moment at room temperature, II) pre-hybridization solution for a moment at room temperature, III) pre-hybridization solution for 45 min at 65 °C.

10 µL of the labeled probe were mixed with 90 µL of distilled H_2O and denatured at 95 °C for 5 min followed by cooling on ice for 2 min. The DNA probes were added to the hybridization solution and hybridized overnight with the nylon membrane at the Tm of the DNA probes minus 5 to 10 °C (see table 5). Subsequently, the nylon membrane was incubated with I) 2X SSC and 0.1% SDS at room temperature for a moment, II) a volume of 2X SSC and 0.1% SDS equivalent to 3-5 volumes of the Pre-hybridization solution for 5 min at room temperature, III) a volume of 2X SSC and 0.1% SDS equivalent to 3-5 volumes of the Pre-hybridization solution for 15 min at the Tm of DNA probes minus 10 to 15 °C, IV) the step III was repeated.

Thereafter, the membrane was dried for 5 min at room temperature, wrapped in a plastic bag, exposed onto a phosphorimager-type screen (Imaging Screen-K; Kodak), and scanned after an exposure of several hours using Molecular Imager FX™ (BioRad).

3.3.5 SDS-PAGE of mitoribosome proteins (mito-r-proteins)

The samples were incubated in 0.1 M DTT, 1X SDS-PAGE loading buffer, and DEPC-treated H_2O at 95 °C for 5 min and run in a 18% SDS-PAGE at 80 mV until the dye was positioned 1 cm before the gel end. The SDS-PAGE was stained for 1 h using Coomassie Brilliant Blue G-250 in 45% methanol and 10% acetic acid while gently shaking. Subsequently, it was first incubated for 1 h with distaining solution while gently shaking and then overnight with the same solution. Finally, it was washed with milli-Q H_2O and the picture was taken using the Gel Doc™ EZ system.

3.4 Mass spectrometry analysis

Samples were concentrated as follows: We loaded fractions enriched in the mt-SSU ribosome on a 10-kDa Amicon® Ultra-0.5 centrifugal filter (Millipore Sigma) and performed centrifugation at 14,000 g for 30 min at 4 °C. The mito-r-proteins remained in the column and the eluate was discarded. The centrifugation in the Amicon® Ultra-0.5 filter unit was repeated until the entire sample was concentrated into 65 µL. Then, the column was placed upside down in a new centrifugation tube and the concentrated mito-r-proteins were recovered by centrifugation at 1,000 g for 2 min at 4 °C.

Proteins were precipitated as follows: The concentrated mito-r-proteins were mixed with UA buffer (for the buffer composition, see appendix 8.2.28) to a final concentration of 6M urea, and loaded on top of a 3-kDa Amicon® Ultra-0.5 centrifugal filter unit followed by centrifugation at 14,000 g until obtaining a sample volume of 100 µl. Then, the sample was mixed with 50 µl of distilled H_2O and 250 µl of UA buffer followed by centrifugation at 14,000 g until obtaining a sample volume of 100 µl. Afterwards, the sample was mixed with 100 µl of distilled H_2O and 200 µl of UA buffer followed by centrifugation at 14,000 g until obtaining a sample volume of 100 µl. Finally, the column was placed upside down in a new centrifugation tube and the concentrated mito-r-proteins were recovered by centrifugation at 1,000 g for 2 min at 4 °C.

Prior to submission to the MS analysis, we quantified the proteins by the Bradford method using a calibration curve of bovine serum albumin (BSA) (table 6 and figure 8). 1 µl of denatured proteins were mixed with 160 µl of Bio-Rad Protein Assay Dye Reagent, and 640 µl of milli-Q H_2O followed by incubation for 5 min at room temperature. The absorbance was measured at 595 nm.

Table 6. BSA standards used in the linear regression analysis for protein quantification.

1 µg/µl BSA	1	2	3	4	5
Abs at 595 nm	0,0695	0,1585	0,1826	0,2417	0,2641

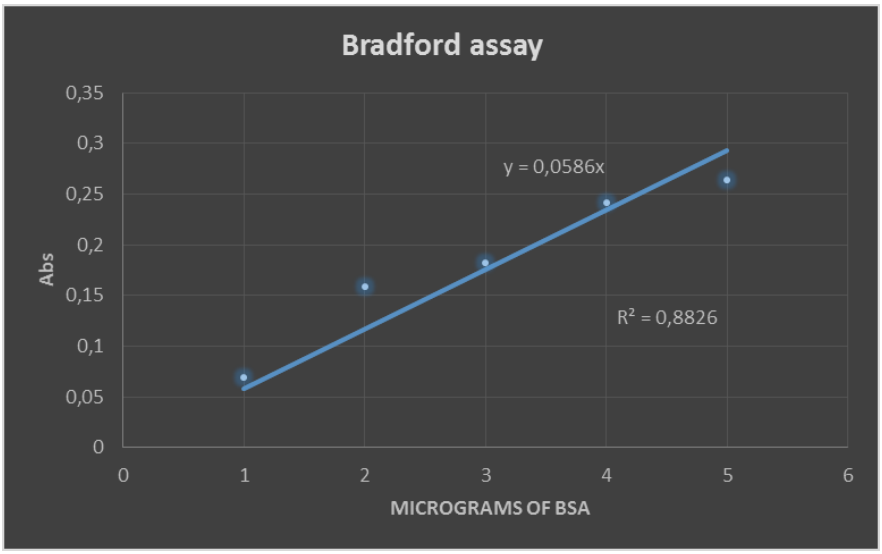

Figure 8. Linear regression analysis performed for protein quantification. *; Y, absorbance at 595 nm; X, µg of BSA; R^2, R squared value.

In-solution trypsin digestion and LC-MS/MS analysis of the peptide mixture were performed at the proteomics platform of the IRCM (Institut de recherches cliniques de Montréal).

3.5 Sequence analysis

MS/MS samples were analyzed with MaxQuant v1.6.1.0 software using the custom database of *A. godoyi* proteins (based on the predicted mitochondrial and nuclear genes), assuming trypsin as the digestion enzyme (96). Spectra were searched with a fragment ion mass tolerance of 0.5 Da and a precursor ion tolerance of 20 ppm. Carbamidomethyl of cysteine was specified as a fixed modification. Oxidation of methionine, deamidation of asparagine or glutamine, phosphorylation of serine, threonine or tyrosine, and conversion of glutamine to pyrrolidonecarboxylic acid (PCA) were specified as variable modifications. Five or less per-peptide modifications were allowed. Minimum and maximum peptide lengths were set to 7 and 25 amino acid residues, respectively, with the molecular weight range from 700 to 4,600 Da. False discovery rate (FDR) for peptide-spectrum matches (PSMs) was set to 1%. As positive protein identifications were considered those for which at least one unique peptide could be assigned with a minimum identification probability above the calculated 1% FDR (false discovery rate).

4. RESULTS

The main objectives of this work were the prediction of the composition of *A. godoyi* mitoribosome using its genomic sequences, experimental characterization of the protein composition in its mt-SSU ribosome, and comparison against its counterpart's composition in the model organisms discussed above.

4.1 Sucrose gradient purification of the *A. godoyi* small subunit mitoribosome

We estimated the enrichment of the small subunit of the mitoribosome (mt-SSU ribosome) based on the quantification of mt-SSU-rRNA in gradient fractions containing protein complexes, because free rRNA does not enter sucrose layers of concentration

superior to 10%. To analyze the enrichment of mt-SSU-rRNA bound to mito-r-proteins, RNA from the gradient fractions was extracted and migrated (see section 3.2).

The jakobid mitochondria is physically associated with other subcellular structures and there are not standardized protocols for its purification (87). Since preliminary purification experiments in our research group showed low yields of mitochondria, we chose to use the sucrose gradient ultracentrifugation to purify the mt-SSU ribosome of *A. godoyi* directly from the whole-cell lysates.

The agarose gel in figure 9 shows the RNA profile across the various sucrose gradient fractions. *A. godoyi* mt-SSU-rRNA (1588 nt) migrates indeed slightly above 1,500 nt, and it is observed in all pooled fractions. The enrichment of mt-SSU-rRNA starts in pool C, with nearly no other RNA species visible. In contrast, the yield is highest in pools F and G, which contain approximately equimolar quantities or even more of cytosolic rRNAs and mt-LSU-rRNA.

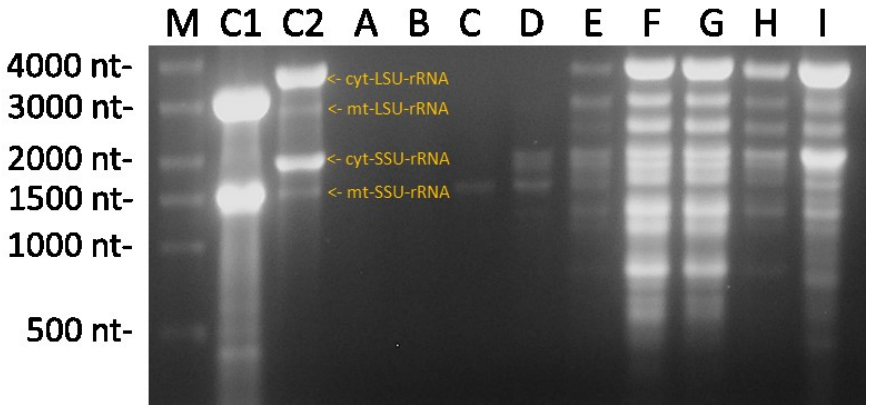

Figure 9. RNA extracted from fractions of a 5 ml 15-40% sucrose gradient. Every two subsequent fractions were pooled. *; mt, mitochondrial; C1, total RNA from *E. aerogenes*; C2, total RNA from *A. godoyi*; A, fractions 1-2; B, 3-4; C, 5-6; D, 7-8; E, 9-10; F, 11-12; G, 13-14; H, 15-16; I, 17-18.

Since *A. godoyi* uses bacteria as a food source, we analyzed the presence of the 16S bt-rRNA to rule out contamination from bacterial ribosomes. The 16S bt-rRNA (1533 nt)

from the food bacterium has a very similar migration behaviour as *A. godoyi* mt-SSU-rRNA. To unambiguously distinguish the two SSU-rRNAs, we performed PCR amplification with specific primers on selected unpooled sucrose-gradient fractions. Figure 10 shows that contaminating SSU-rRNAs occur in fractions 8 and higher. The evidences of Figures 9 and 10 combined demonstrate that *A. godoyi* mt-SSU-rRNA is the purest in fractions 5 to 7.

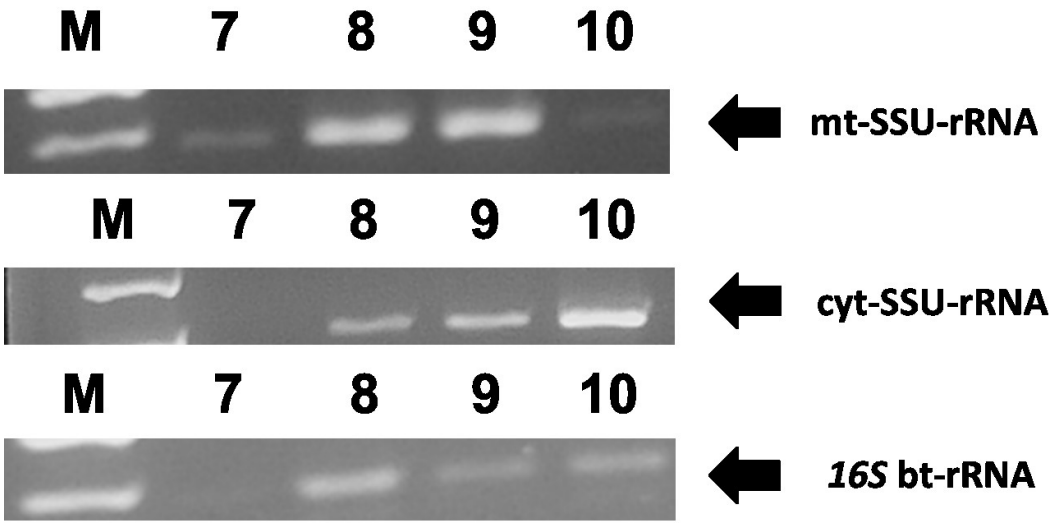

Figure 10. Amplification of SSU-rRNAs in single gradient fractions. Primers ag06 + ag05 were used for mt-SSU-rRNA, NS5-fwd + BMB-C-rev for cyt-SSU-rRNA, and ag06 + eb04 for 16S bt-rRNA (See appendix 8.3). *; M, marker; mt, mitochondrial; cyt, cytosolic; bt, bacterial. 7-10 individual gradient fractions.

4.2 Validating the enrichment of *A. godoyi* mt-SSU-rRNA

Northern hybridization served as the final validation of mt-SSU ribosome enrichment in sucrose gradient fractions. For that, we used RNA extracted from the pooled gradient fractions (see table 4) and probes specific for the 16S bt-rRNA, 23S bt-rRNA, mt-SSU-rRNA, and the mt-LSU-rRNA (see the table 5 and the appendix 8.4). The fractions 5 and 6 were enriched in the mt-SSU ribosome of *A. godoyi* (see section 4.1).

A strong signal for 16S bt-rRNA and 23S bt-rRNA was detected using the probes eb02 and eb03 in *Enterobacter* total RNA (figure 11). We detected a weak signal in *Andalucia* total RNA and in the heavier gradient fractions, which may be due to non-specific cross hybridization of probes eb02 and eb03 with the cyt-rRNAs. Non-specific cross hybridization can be observed in the RNA marker as well. The gradient fractions 1-12 were free from bacterial ribosomes because we did not detect any hybridization signal in the fraction pools A-F (figure 11).

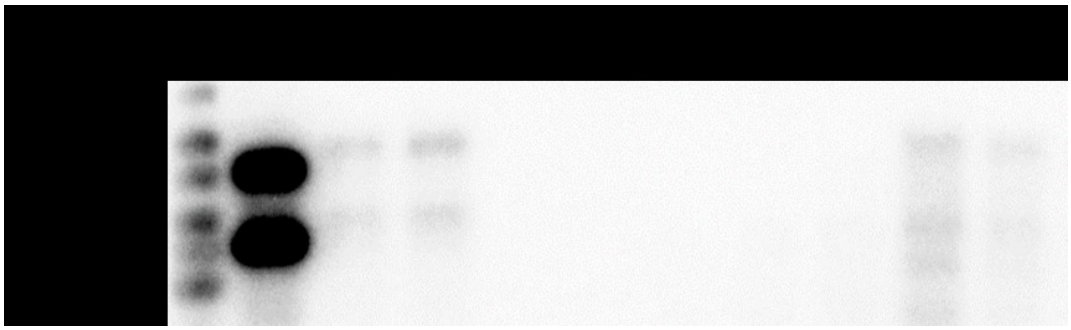

Figure 11. The enrichment of the 16S bt-rRNA and the 23S bt-rRNA was analyzed by Northern blot (see figure 9). The probes eb02 and eb03 were used for detection of 16S bt-rRNA and 23S bt-rRNA, respectively (See appendix 8.4). R1, *Enterobacter* total RNA; R2-R3, *Andalucia* total RNA; A-H, pooled gradient fractions (see the legend of the figure 9).

A strong signal representing the mt-SSU-rRNA was detected using the probe ag03 with *Andalucia* total RNA (figure 12). A weak non-specific cross hybridization can be detected in the RNA marker as well. We did not detect any hybridization signal in the fraction pools A-B. The mt-SSU ribosome is enriched in the pools C and D (fractions 5-8) because the peak of the mt-SSU-rRNA started at the fraction pool C and the strongest signal was detected in the pool D (figure 12). However, we chose only the pool C for the characterization of the mt-SSU ribosome to avoid contamination with *Andalucia* cyt-SSU-rRNA contained in the gradient fraction 8 (pool D) (see figure 9).

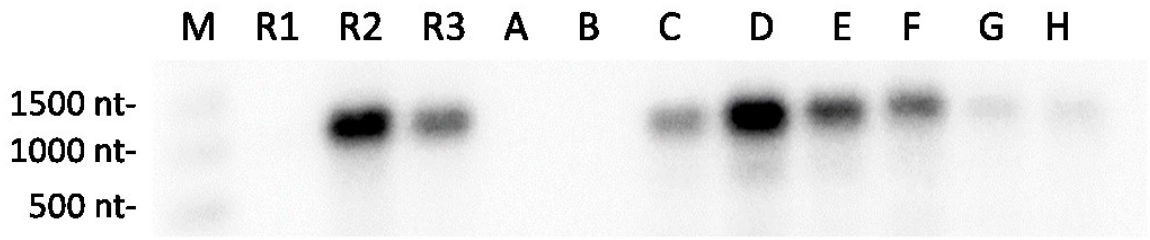

Figure 12. The enrichment of the mt-SSU-rRNA was quantified by Northern blot (see figure 9)**.** The probe ag03 was used for mt-SSU-rRNA detection (see appendix 8.4). R1, *Enterobacter* total RNA; R2-R3, *Andalucia* total RNA; A-H, gradient fraction pools (see the legend of the figure 9).

A strong signal for the mt-LSU-rRNA was detected in *Andalucia* total RNA using the probe ag04 (figure 13), but not in fraction pools A-E. The upmost fraction containing the mt-LSU-rRNA is pool F and the strongest signal was detected in pool G (figure 13).

Figure 13. The enrichment of the mt-LSU-rRNA was analyzed by Northern blot (see figure 9)**.** The probe ag04 was used for 16S mt-rRNA detection (See appendix 8.4). R1, *Enterobacter* total RNA; R2-R3, *Andalucia* total RNA; A-H, gradient fraction pools (see the legend of the figure 9).

We finally analysed the profile of protein bands in the gradient fractions 5-6 (see figure 9), which turned out to differ considerably from the profile in the whole-cell lysate (figure 14). Moreover, the protein concentration in these gradient fractions appears to be smaller than in the whole-cell lysate. We infer that the concentration of cytoplasmic proteins is lower in the gradient fractions where the mt-SSU ribosome is enriched.

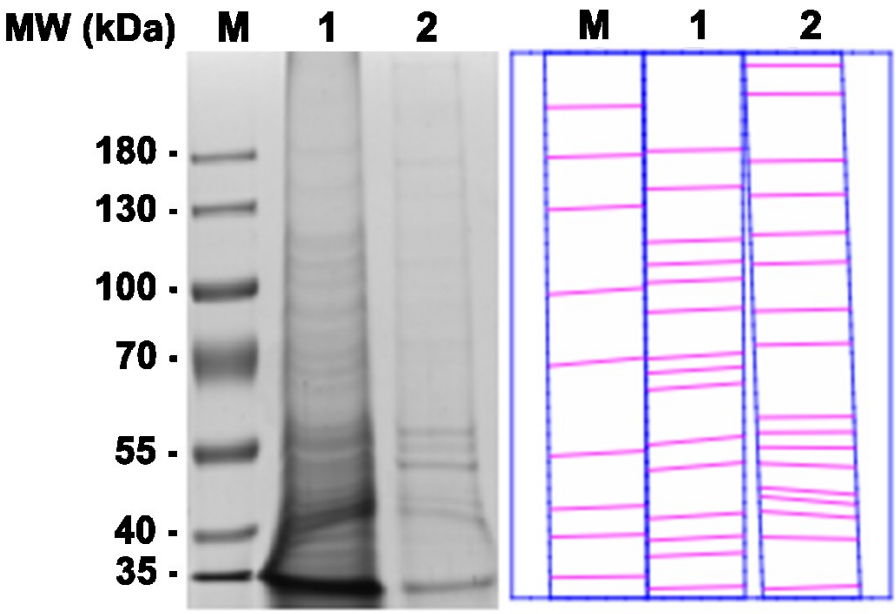

Figure 14. Protein electrophoresis. M, protein marker; 1, whole-cell lysate of *A. godoyi*; 2, proteins from fractions 5-6 (see figure 9). The grid of detected protein bands by the Image Lab™ software is shown on the right.

4.3 Mass spectrometry analysis and comparison with predicted SSU mito-r-proteins

It is known that small polar proteins can be easily lost during the purification of ribosomes (97). Therefore, we compared the protein composition in the mt-SSU ribosome of *A. godoyi in silico*.

Michael W. Gray kindly provided the annotation of nucleus-encoded mito-r-proteins of *A. godoyi*. Then, we compiled this protein set with previously annotated mitochondrion-encoded mito-r-proteins (15), strongly suggesting that *Andalucia*'s mitoribosome contains 69 mito-r-proteins, of which 28 belong to the mt-SSU ribosome and 41 to the mt-LSU ribosome (table 7).

Table 7. Mito-r-proteins inferred from the *A. godoyi* nuclear and mitochondrial genome sequences.

Small subunit (mt-SSU)		Large subunit (mt-LSU)	
S1	S25	L1	L24
S2	S29	L2	L25
S3	S33	L3	L27
S4	S35	L4	L28
S5	Rsm22	L5	L29
S6	Ppe1	L6	L31
S7	Mrp10	L9	L32
S8		L10	L33
S9		L11	L34
S10		L12	L35
S11		L13	L36
S12		L14	L38
S13		L15	L40
S14		L16	L41
S15		L17	L43
S16		L18	L45
S17		L19	L46
S18		L20	L49
S19		L21	L53
S21		L22	L54
S23		L23	

*; mito-r-proteins, mitoribosome proteins.

Trypsin digestion and analysis by LC-MS/MS allowed detection of each mito-r-protein predicted to be part of the mt-SSU ribosome of *A. godoyi* (table 8) with at least two unique peptides in the gradient fraction enriched with the mt-SSU ribosome. The only exceptions were S25 and Ppe1, for which, in this experiment, we did not detect peptides. Still, an earlier MS experiment performed on lysates of a subcellular fraction enriched in mitochondria reported multiple peptides of the S25 protein (though none for Ppe1). Table 8 compares the sets of mito-r-proteins across different organism, employing the unified nomenclature for mito-r-proteins proposed by (98).

Table 8. Proteins in the small subunit of the mitoribosome.

New name [a] (98)	Yeast (64, 72)	Human (98)	Bacteria (98)	*A. godoyi* : genome-sequence inferred	*A. godoyi* : MS/MS	*Trypanosome* (63, 66, 67)	*Leishmania* (75) (63)	Plant (99, 100)
bS1	-	MRPS28	S1	S1	S1	-	-	-
uS2	Mrp4	MRPS2	S2	S2	S2 [b]	-	-	S2
uS3	Var1?	MRPS24	S3/S24	S3	S3	-	-	S3
bS4	Nam9	-	S4	S4	S4[b]	-	-	S4
uS5	Mrps5	MRPS5	S5	S5	S5[b]	S5	S5	S5
bS6	Mrp17	MRPS6	S6	S6	S6[b]	S6	S6	S6
uS7	Rsm7	MRPS7	S7	S7	S7	-	-	S7
bS8	Mrps8	-	S8	S8	S8[b]	S8	S8	S8
bS9	Mrps9	MRPS9	S9	S9	S9[b]	S9	S9	S9
uS10	Rsm10	MRPS10	S10	S10	S10[b]	-	-	S10
uS11	Mrps18	MRPS11	S11	S11	S11	S11	S11	S11
uS12	Mrps12	MRPS12	S12	S12	S12	S12	-	S12
bS13	Sws2	-	S13	S13	S13[b]	-	-	S13
uS14	Mrp2	MRPS14	S14	S14	S14[b]	-	-	S14
uS15	Mrps28	MRPS15	S15	S15	S15[b]	S15	S15	S15
bS16	Mrps16	MRPS16	S16	S16	S16[b]	S16	S16	S16
uS17	Mrps17	MRPS17	S17	S17	S17	S17	S17	-
-	-	-	-	-	-	-	-	S17B
-	-	-	-	-	-	-	-	S17C
-	-	-	-	-	-	-	-	S17D
mS18b	-	MRPS18-2	S18	-	-	-	-	-
bS18c	Rms18	MRPS18-1	S18	S18	S18	S18	S18	S18
uS19	Rsm19	-	S19	S19	S19[b]	-	-	S19
bS21	Mrp21	MRPS21	S21	S21	S21[b]	-	-	-
uS22	-	MRPS22	S22	-	-	-	-	-
uS23	Rsm25	MRPS23	S23	S23	S23[b]	-	-	-
mS25	Mrp49	MRPS25	-	S25	S25[c]	-	-	-
mS26	-	MRPS26	-	-	-	-	-	-
mS27	-	MRPS27	-	-	-	-	-	-
mS29	Rsm23	MRPS29	-	S29	S29[b]	S29	S29	S29
mS31	-	MRPS31	-	-	-	-	-	-
mS33	Rsm27	MRPS33	-	S33	S33[b]	-	-	-
mS34	-	MRPS34	-	-	-	S34	S34	-
mS35	Rsm24	MRPS35	-	S35	S35[b]	-	-	-
mS36	Ymr31	MRPS36	-	-	-	-	-	-

(Continues in the next page)

New name [a]	Yeast	Human	Bacteria	*A. godoyi* : genome-sequence inferred	*A. godoyi* : MS/MS	*Trypanosome*	*Leishmania*	Plant
mS37	-	MRPS37	-	-	-	-	-	-
mS38	Cox24	MRPS38	-	-	-	-	-	-
mS39	-	MRPS39	-	-	-	-	-	-
mS40	Rsm22	-	-	Rsm22	Rsm22	Rsm22	Rsm22	-
mS41	Mrps35	-	-	-	-	-	-	-
mS42	Mrp51	-	-	-	-	-	-	-
mS43	Mrp13	-	-	-	-	-	-	-
mS44	Mrp1	-	-	-	-	-	-	-
mS45	Pet123	-	-	-	-	-	-	-
mS46	Rsm26	-	-	-	-	-	-	-
mS47	Mrp10	-	-	Mrp10	Mrp10	-	-	-
mS48	Rsm28	-	-	-	-	-	-	-
mS49	Ppe1	-	-	Ppe1	-	Ppe1	Ppe1	-

[a] The ribosome community proposed a unifying nomenclature for mito-r-proteins, which uses the prefix "b" for bacterial proteins that lack a eukaryotic or archaeal homolog, the prefix "u" for proteins observed in all kingdoms of life, and the prefix "m" for mitochondrion-specific proteins. Modified from (98). *; mito-r-proteins, mitoribosome proteins

[b] Detected in the mtSSU-enriched fraction of the total cell lysate and in the mitochondrial lysate.

[c] Only detected in the mitochondrial lysate, but not in the mtSSU-enriched fraction.

The mt-SSU ribosome of *A. godoyi* is composed of at least 27 proteins (figure 15), a number which is larger than in the SSU of *E. coli* (21 proteins), but smaller than in the mt-SSU ribosome of *S. cerevisiae* (36 proteins), *H. sapiens* (31 proteins), *T. brucei* (58 proteins), and *L. tarantolae* (20 proteins). Of these 27 proteins in the mt-SSU ribosome of *A. godoyi*, 21 are homologs of bacterial r-proteins (figure 16), which is more than in the mt-SSU ribosome of all model organism, notably *S. cerevisiae* (20 proteins), *H. sapiens* (18 proteins), A. *thaliana* (17 proteins), *T. brucei* (9 proteins), and *L. tarantolae* (10 proteins). In turn, the number of eukaryote-specific mito-r-proteins in *A. godoyi* mt-SSU ribosome is six, which is smaller than in its counterparts from *S. cerevisiae* (16 proteins) and *H. sapiens* (13 proteins), but larger than in its counterparts in *A. thaliana* (one protein), and *T. brucei* and *L. tarantolae* (4 proteins) (figure 17).

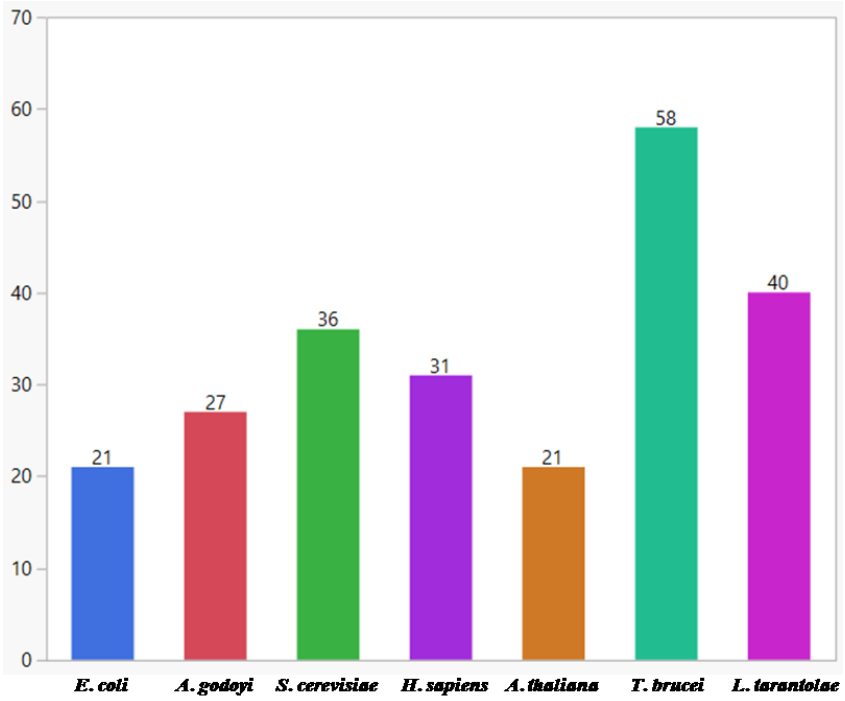

Figure 15. Total number of proteins in the SSU of *E. coli* and the mt-SSU ribosome of select eukaryotes. *; SSU, small subunit of the ribosome; mt-SSU, small subunit of the mitoribosome.

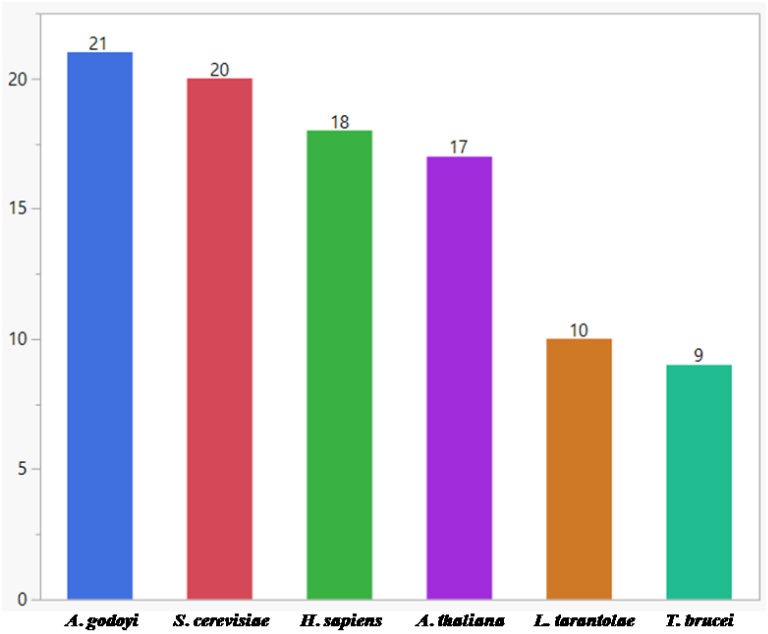

Figure 16. Number of bacterial homolog proteins in the mt-SSU ribosome of different organisms. *; mt-SSU, small subunit of the mitoribosome.

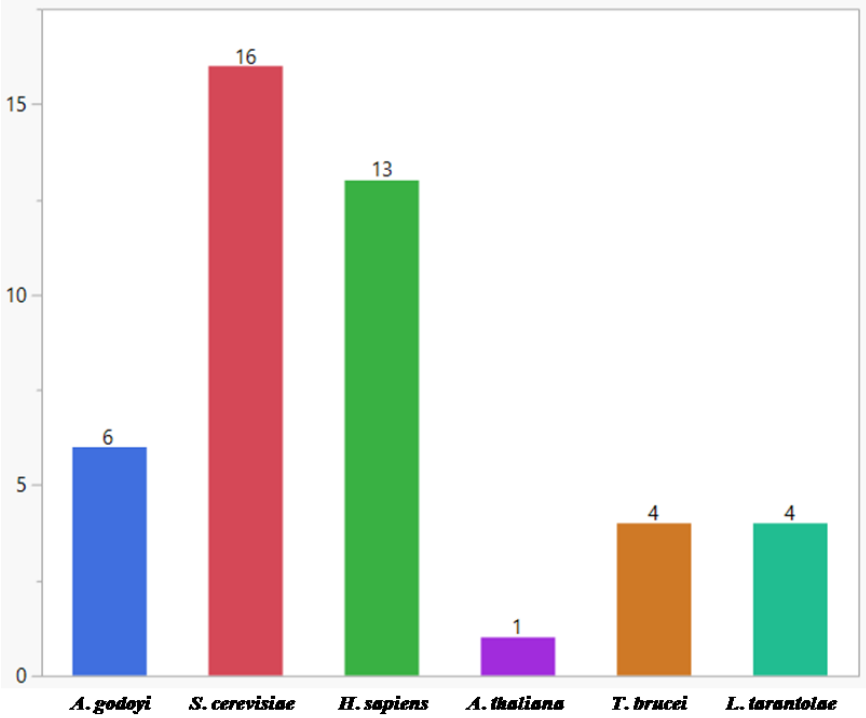

Figure 17. Number of eukaryotic-specific proteins in the mt-SSU ribosome of different organisms. *; mt-SSU, small subunit of the mitoribosome.

4.4 Additional proteins detected in the mt-SSU ribosomal fraction of *Andalucia godoyi*

As described above, we detected 27 bona-fide mito-r-proteins in our preparation of enriched *Andalucia* mt-SSU ribosome. In addition to these, the preparation contained also 133 proteins annotated as "hypothetical proteins" in the database of genome-inferred *Andalucia* proteins. These hypothetical proteins had the same range of peptide coverage in MS/MS (i.e., 5 to 27) as the conserved mito-r-proteins, but did not share significant similarity with any known protein. It is currently uncertain, whether these proteins are indeed part of the mt-SSU ribosome or rather of another complex that fortuitously co-sedimented with the former in sucrose gradient separation.

4.5 Tracing the evolutionary history of SSU mitoribosomal proteins in Discoba

The mt-SSU ribosome of the last Bikont ancestor was predicted to possess 28 mito-r-proteins and to have subsequently lost, S21, S23, S33, S35, S36, and Mrp10 during the diversification of the lineage that leads to the Discoba (previously known as Excavata), leaving 22 mito-r-proteins at the basis of this clade (63). However, a new picture arose when the prediction of mito-r-proteins in the ancestor of Discoba was refined using the set of mito-r-proteins inferred from genome sequences of *A. godoyi* (analysis performed by MW. Gray; table 9). Now, the mt-SSU ribosome of this ancestor is predicted to have possessed the same mito-r-protein set as the Bikont ancestor with only one difference, notably S36, which was lost during the diversification of the linage leading to the Discoba. The mt-SSU ribosome of the ancestor of the latter contains fewer mito-r-proteins than its counterpart in the ancestor of animals (30 mito-r-proteins) and fungi (31 mito-r-proteins), which already possessed a significantly remodeled mt-SSU ribosome. Mrp10 was likely lost in the branch that lead to non-jakobid groups of Discoba, as it is present in the mt-SSU ribosome of *A. godoyi,* but absent in the mt-SSU ribosome of other Discoba members.

Table 9. Inference of the set of mito-r-proteins present in the mt-SSU ribosome of the last common ancestor of Discoba[a].

Nucleus-encoded	Mitochondrion-encoded
S5, S6, S9, S15, S16, S17, S18, S21, S23, S25, S29, S33, S34, S35, Rsm22, Mrp10	S1, S2, S3, S4, S7, S8, S10, S11, S12, S13, S14, S19

[a]Names of newly inferred proteins are underscored (MW. Gray, unpublished).

5. DISCUSSION

The mitoribosome underwent drastic changes during eukaryotic evolution, featuring novel proteins and shortened rRNAs (59). Specifically, the small subunit of the mitoribosome (mt-SSU ribosome), which contains the mt-mRNA entrance channel, was extensively remodeled, apparently to adapt to the particularities of mitochondrial protein synthesis and mitochondrial mRNAs. To get insight into mt-SSU ribosome evolution, we analyzed the composition of this subunit from *A. godoyi*, a free-living jakobid that contains the most bacteria-like mitochondrial genome currently known (15, 85), which made us assume that the mitoribosome is less divergent compared to that of other eukaryotes.

5.1 Technical challenges in the purification of *A. godoyi* mt-SSU ribosome

This project was not without unexpected technical challenges. Obtaining enough cellular material was time consuming because *A. godoyi* has a replication time of 32-48 hr and reaches the stationary phase already at $1.875x10^6$ cells/ml. Since the preliminary experiments in our research group showed that the yield of mitochondria is too small for the characterization of the *Andalucia's* mitoribosome, we attempted purification of the mitoribosome from whole-cell lysates. However, the mt-LSU ribosome could not be separated from the cytosolic ribosome in sucrose gradient ultracentrifugation, and therefore, this subunit was not suited for further examination. In contrast, we succeeded to obtain by this method a fraction highly enriched in the mt-SSU ribosome that we investigated in detail.

5.2 Identification and analysis of SSU mitoribosomal proteins from *A. godoyi*

Mass spectrometry analysis of the enriched mt-SSU ribosome preparation identified nearly all of the mito-r-proteins predicted from the *A. godoyi* nuclear and mitochondrial genomes

(26 out of 28 mito-r-proteins) with the exception of S25 and Ppe1. S25, which was detected in MS analyses of whole mitochondrial lysates in a previous experiment in our research group is a mitochondrion-specific r-protein, which is located at the periphery of mammalian mitoribosomes (35). If S25 of *Andalucia* is also located at the periphery of the mitoribosome, this might explain why it has been lost during the purification procedure. The same phenomenon has been observed with the proteins S1 and L9 during the purification of bacterial ribosomes (97). The second missing protein, Ppe1, was traditionally thought to be a constituent of yeast mitoribosomes (79). As it has not been identified in the most recent structural studies, it is now thought to be only transiently associated with the mt-SSU ribosome (72). The same may apply to Ppe1 of *A. godoyi*, because it was not detected either in samples enriched in mt-SSU ribosomes or in whole mitochondrial lysates.

Thus, in sum, we succeeded to validate experimentally 27 out of the 28 mito-r-proteins, confirming that the mt-SSU ribosome of *A. godoyi* contains the most conserved core of mito-r-proteins currently known, harboring more bacterial homologs than its counterparts in yeast, mammals, kinetoplastids, and plants, and at the same time containing fewer mitochondrion-specific r-proteins than any other eukaryote studied so far.

5.3 The composition of *A. godoyi* mt-SSU ribosome

There is apparently no correlation between the size of mt-rRNAs and the number of mito-r-proteins (59). Nonetheless, the sequence similarity of mt-rRNAs with bacterial rRNAs may be correlated with the number of bacterial-like r-proteins. For instance, *Andalucia* mt-SSU-rRNA has a high degree of sequence similarity with *E. coli* 16S rRNA and possess more bacteria-like r-proteins than its mammalian counterpart. The same phenomenon has been observed, but to a lesser extent in the mt-SSU ribosome of yeast (72).

The mt-SSU ribosome of *A. godoyi* appears to be at a more primitive stage in the evolutionary process of mito-r-proteins recruitment because its total protein number is smaller than that of other eukaryotes. However, as of now, we cannot discard the presence

of clade-specific mito-r-proteins in *A. godoyi*, since the structure of its mitoribosome has not been determined, which would allow to distinguish fortuitous proteins present in our preparation and genuinely novel components of this ribosome.

5.4 Evolution of protein composition in the mt-SSU ribosome of *Discoba*

The analysis of genomic sequences of *A. godoyi* allowed us to refine the predicted set of mito-r-proteins in the ancestor of Discoba. The linage that lead to the ancestor of Discoba may have split very rapidly from the Bikont ancestor because only the mito-r-protein S36 was lost during this evolutionary transition. Then, the linage leading to jakobids probably remained evolutionary stagnant, whereas other clades within Discoba, most drastically exemplified by kinetoplastids, lost numerous homologs of bacterial r-proteins. The mt-SSU ribosome of *Naegleria gruberi*, another member of Discoba, did not lose as many homologs of bacterial mito-r-proteins as that of kinetoplastids, however it is not as conserved as its counterpart in *A. godoyi* (63).

The mt-SSU ribosome of the ancestors of Archaeplastida and Discoba contains the same protein number (27 mito-r-proteins) and an almost identical mito-r-protein set. The only differences are S25 that is absent in the ancestor of Archaeplastida, and S26 that is absent in the ancestor of Discoba. Since the mt-SSU ribosome contains the mt-mRNA entrance channel that is required for translation initiation, both ancestors likely possessed a similar mechanism of mitochondrial translation initiation. Further, the mitochondria of both ancestors probably possessed similar target sequences for the recruitment of mt-mRNAs to the mt-SSU ribosome, and a similar number and structure of initiation factors. Moreover, both ancestors likely had comparable mechanisms of translation initiation steps such as mt-mRNA recruitment, recognition of initiation triplets, recruitment of mt-tRNAs, and the association of both mitoribosome subunits.

6. OUTLOOK AND FUTURE WORK

We confirmed experimentally the predicted protein composition of the *A. godoyi* mt-SSU ribosome and compared it with the protein composition of the bacterial SSU and the mt-SSU ribosome of more divergent eukaryotes. Bacterial rRNAs have a higher base paring conservation of secondary, tertiary, and A-minor interaction sites than mt-rRNAs (59). In order to determine in how far the arrangement of proteins and rRNA in this ribosome deviates from bacteria on one side and model eukaryotes on the other, we need to determine the structure of the *Andalucia* mt-SSU ribosome, e.g., by cryo-Electron Microscopy (cryo-EM) (101). However, a prerequisite to this approach is the establishment of protocols that allow the isolation of mitochondria in sufficient quantity and quality, which are currently not in place.

The functional innovation of mt-rRNAs could be studied through mutation or insertion of expansion segments in the mt-rRNA sequences. However, protocols for genetic manipulations are currently not available for any jakobid (15).

Although the global composition of *Andalucia* mt-SSU ribosome resembles its bacterial counterpart, it would be interesting to analyze if the individual mito-r-proteins themselves are more bacterial-like or eukaryotic-like. This can be achieved by comparing the sequence similarity and the functional domains of each protein in the *Andalucia* mt-SSU ribosome with its bacterial and eukaryotic counterparts. Moreover, the degree of hydrophobicity and the PI of each mito-r-protein could be compared with their values in counterparts from other organisms.

Another interesting avenue would be to identify nucleotide modifications of *Andalucia* mt-SSU-rRNA. In particular, it has been shown in model organisms that methylation at specific rRNA positions is required for the assembly and stability of the mitoribosome. Rsm22, which is associated with the ribosomal SSU, seems to catalyze this reaction (102-104).

To assess ribosome remodelling during eukaryotic evolution, we could employ an *in silico* approach, whereby N- and C-terminal extensions of mito-r-proteins will be

identified to compare their sizes across different organisms. These extensions are believed to have allowed deletions to different degrees in several segments of the mt-rRNAs. We expect that the size of N- and C- terminal extensions in conserved proteins of the mt-SSU ribosome of *A. godoyi* is smaller than that of their homologs in the mt-SSU ribosome of highly diverged eukaryotes.

Another aspect worth examining is the degree of protein interconnectivity in the mitoribosome. The mammalians mito-r-proteins S6, S16, S18, S25, L10, and L66 possess zinc-binding motifs involved in protein interconnectivity. On the other hand, the bacterial homologs of these proteins lack zinc-binding motifs, and the overall number of these motifs in the *E. coli* ribosome is smaller compared to the mammalian mitoribosome (105). The identification of zinc binding motifs in mito-r-proteins would allow to test the hypothesis that the structure of *Andalucia*'s mitoribosome has a lesser degree of protein interconnectivity compared to the mitoribosome of more divergent eukaryotes.

In addition to the shared set of eukaryotic-specific mito-r-proteins, the mitoribosomes of *S. cerevisiae*, *H. sapiens*, *T. brucei*, and *L. tarantolae* contain several organism-specific mito-r-proteins. The mt-SSU ribosome preparation from *A. godoyi* also contains several additional proteins that do not share significant similarity with any known ribosomal protein. Highly sensitive *in silico* analysis will be required such as searches with profile Hidden Markov Models to assess the potential of these components to constitute indeed unique components of the *Andalucia*'s mitoribosome (106). Moreover, computational prediction of mitochondrial import signals and experiments to test protein import into isolated yeast mitochondria could corroborate mitochondrial localization (107, 108). Furthermore, we could study the regulation of the mitoribosome composition by analysing the mt-SSU ribosome of *Andalucia* cultivated under stress or perturbation conditions that alter mitochondrial translation. Such experiments will most likely allow refining the list of potential novel mito-r-proteins.

Finally, we need to determine if the features of the *Andalucia* mitoribosomal SSU are indeed (as we assumed throughout this thesis) shared by all jakobids or are specific characteristics of *A. godoyi*. While the former view is corroborated by preliminary analyses

of genome sequences from several *Jakoba* and *Reclinomonas* species, a comprehensive comparison is needed to give a definitive answer.

Traditionally, the evolution of the mitoribosome has been investigated by comparing the composition of bacterial ribosomes with the mitoribosome composition of highly diverged eukaryotes such as mammals and yeast. Our work is an attempt to characterize mitoribosomes from more primitive eukaryotes, and therefore could help us to refine our understanding of the early and intermediate stages in the evolution of the mitochondrial translation machinery.

7. REFERENCES

1. McBride HM, Neuspiel M, Wasiak S. Mitochondria: More than just a powerhouse. Curr Biol. 2006;16(14):R551–R60.
2. Flegontov P, Michálek J, Janouškovec J, Lai DH, Jirků M, Hajdušková E, et al. Divergent mitochondrial respiratory chains in phototrophic relatives of apicomplexan parasites. Mol Biol Evol. 2015;32(5):1115-31.
3. Timmis JN, Ayliffe MA, Huang CY, Martin W. Endosymbiotic gene transfer: organelle genomes forge eukaryotic chromosomes. Nat Rev Genet. 2004 5(2):123-35.
4. Maier UG, Zauner S, Woehle C, Bolte K, Hempel F, Allen JF, et al. Massively convergent evolution for ribosomal protein gene content in plastid and mitochondrial genomes. Genome Biol Evol. 2013;5(12):2318-29.
5. Allen JF, Raven JA. Free-radical-induced mutation vs redox regulation: costs and benefits of genes in organelles. J Mol Evol. 1996;42(5):482-92.
6. Lynch M, Koskella B, Schaack S. Mutation pressure and the evolution of organelle genomic architecture. Science. 2006;311(5768):1727-30.
7. Doolittle WF. You are what you eat: a gene transfer ratchet could account for bacterial genes in eukaryotic nuclear genomes. Trends Genet. 1998;14(8):307-11.
8. Martin W, Herrmann RG. Gene transfer from organelles to the nucleus: how much, what happens, and why? Plant Physiol. 1998;118(1):9-17.
9. Cavalier-Smith T. Kingdoms protozoa and chromista and the eozoan root of the eukaryotic tree. Biol Lett. 2010 Jun;6(3):342-5.
10. Hazkani-Covo E, Covo S. Numt-mediated double-strand break repair mitigates deletions during primate genome evolution. PLoS Genet. 2008;4(10):e1000237.
11. Hazkani-Covo E, Zeller RM, Martin W. Molecular poltergeists: mitochondrial DNA copies (numts) in sequenced nuclear genomes. PLoS Genet. 2010;16(2):e1000834.
12. Björkholm P, Harish A, Hagström E, Ernst AM, Andersson SG. Mitochondrial genomes are retained by selective constraints on protein targeting. Proc Natl Acad Sci U S A. 2015;112(33):10154-61.
13. de Grey AD. Forces maintaining organellar genomes: is any as strong as genetic code disparity or hydrophobicity? Bioessays. 2005 27(4):436-46.

14. Mokranjac D. Mitochondrial protein import: An unexpected disulfide bond. J Cell Biol. 2016;214(4):363-5.
15. Burger G, Gray MW, Forget L, Lang BF. Strikingly bacteria-like and gene-rich mitochondrial genomes throughout jakobid protists. Genome Biol Evol. 2013;5(2):418-38.
16. Greber BJ, Ban N. Structure and function of the mitochondrial ribosome. Annu Rev Biochem. 2016;85:103-32.
17. Valach M, Burger G, Gray MW, Lang BF. Widespread occurrence of organelle genome-encoded 5S rRNAs including permuted molecules. Nucleic Acids Res. 2014;42(22):13764-77.
18. Institute NHGR. Talking Glossary of Genetic Terms: National Institutes of Health; 2018. Available from: https://www.genome.gov/glossary/.
19. Agirrezabala X, Frank J. Elongation in translation as a dynamic interaction among the ribosome, tRNA, and elongation factors EF-G and EF-Tu. Quarterly Reviews of Biophysics. 2009;42(3):159-200.
20. Chen J, Tsai A, O'Leary SE, Petrov A, Puglisi JD. Unraveling the dynamics of ribosome translocation. Curr Opin Struct Biol. 2012;22(6):804-14.
21. Dunkle JA, Cate JH. Ribosome structure and dynamics during translocation and termination. Annu Rev Biophys. 2010;39:227-44.
22. Frank J, Gonzalez RL. Structure and dynamics of a processive Brownian motor: the translating ribosome. Annu Rev Biochem. 2010;79:381-412.
23. Milón P, Rodnina MV. Kinetic control of translation initiation in bacteria. Crit Rev Biochem Mol Biol. 2012;47(4):334-48.
24. Rodnina MV, Wintermeyer W. Fidelity of aminoacyl-tRNA selection on the ribosome: kinetic and structural mechanisms. Annu Rev Biochem. 2001;70:415-35.
25. Chen J, Choi J, O'Leary SE, Prabhakar A, Petrov A, Grosely R, et al. The molecular choreography of protein synthesis: translational control, regulation, and pathways. Q Rev Biophys. 2016;49:e11.
26. Rossmanith W. Localization of human RNase Z isoforms: dual nuclear/mitochondrial targeting of the ELAC2 gene product by alternative translation initiation. PLoS One. 2011;6(4):e19152.
27. Holzmann J, Frank P, Löffler E, Bennett KL, Gerner C, Rossmanith W. RNase P without RNA: identification and functional reconstitution of the human mitochondrial tRNA processing enzyme. Cell. 2008;135(3):462-74.
28. Tomecki R, Dmochowska A, Gewartowski K, Dziembowski A, Stepien PP. Identification of a novel human nuclear-encoded mitochondrial poly(A) polymerase. Nucleic Acids Res. 2004;32(20):6001-14.
29. Temperley R, Richter R, Dennerlein S, Lightowlers RN, Chrzanowska-Lightowlers ZM. Hungry codons promote frameshifting in human mitochondrial ribosomes. Science. 2010;327(5963):301.
30. Temperley RJ, Wydro M, Lightowlers RN, Chrzanowska-Lightowlers ZM. Human mitochondrial mRNAs--like members of all families, similar but different. Biochim Biophys Acta. 2010;1797(6-7):1081-5.
31. Christian BE, Spremulli LL. Mechanism of protein biosynthesis in mammalian mitochondria. Biochim Biophys Acta. 2012;1819(9-10):1035-54.
32. Ott M, Amunts A, Brown A. Organization and regulation of mitochondrial protein synthesis. Annu Rev Biochem. 2016;2(85):77-101.
33. Mai N, Chrzanowska-Lightowlers ZM, Lightowlersn RN. The process of mammalian mitochondrial protein synthesis. Cell Tissue Res 2017;367(1):5-20.

34. Tucker EJ, Hershman SG, Köhrer C, Belcher-Timme CA, Patel J, Goldberger OA, et al. Mutations in MTFMT underlie a human disorder of formylation causing impaired mitochondrial translation. Cell Metab. 2011;14(3):428-34.
35. Amunts A, Brown A, Toots J, Scheres SH, Ramakrishnan V. Ribosome. The structure of the human mitochondrial ribosome. Science. 2015;348(6230):95-8.
36. Greber BJ, Bieri P, Leibundgut M, Leitner A, Aebersold R, Boehringer D, et al. Ribosome. The complete structure of the 55S mammalian mitochondrial ribosome. Science 2015;348(6232):308-8.
37. Bhargava K, Templeton P, Spremulli LL. Expression and characterization of isoform 1 of human mitochondrial elongation factor G Protein Expr Purif. 2004;37(2):368–76.
38. Soleimanpour-Lichaei HR, Kühl I, Gaisne M, Passos JF, Wydro M, Rorbach J, et al. mtRF1a is a human mitochondrial translation release factor decoding the major termination codons UAA and UAG. Mol Cell. 2007;27(5):745-57.
39. Young DJ, Edgar CD, Murphy J, Fredebohm J, Poole ES, Tate WP. Bioinformatic, structural, and functional analyses support release factor-like MTRF1 as a protein able to decode nonstandard stop codons beginning with adenine in vertebrate mitochondria. RNA. 2010;16(6):1146-55.
40. Rorbach J, Richter R, Wessels HJ, Wydro M, Pekalski M, Farhoud M, et al. The human mitochondrial ribosome recycling factor is essential for cell viability. Nucleic Acids Res. 2008;36(18):5787-99.
41. Tsuboi M, Morita H, Nozaki Y, Akama K, Ueda T, Ito K, et al. EF-G2mt is an exclusive recycling factor in mammalian mitochondrial protein synthesis. Mol Cell. 2009;35(4):502-10.
42. Pfeffer S, Woellhaf MW, Herrmann JM, Förster F. Organization of the mitochondrial translation machinery studied in situ by cryoelectron tomography. Nat Commun. 2015;6:6019.
43. Fox TD. Mitochondrial protein synthesis, import, and assembly. Genetics. 2012;192(4):1203-34.
44. Williams EH, Butler CA, Bonnefoy N, Fox TD. Translation initiation in *Saccharomyces cerevisiae* mitochondria: functional interactions among mitochondrial ribosomal protein Rsm28p, initiation factor 2, methionyl-tRNA-formyltransferase and novel protein Rmd9p. Genetics. 2007;175(3):1117-26.
45. Liao HX, Spremulli LL. Identification and initial characterization of translational initiation factor 2 from bovine mitochondria. J Biol Chem. 1990;265(23):13618-22.
46. Koc EC, Spremulli LL. Identification of mammalian mitochondrial translational initiation factor 3 and examination of its role in initiation complex formation with natural mRNAs. J Biol Chem. 2002;277(38):35541-9.
47. Funes S, Kauff F, Van der Sluis EO, Ott M, Herrmann JM. Evolution of YidC/Oxa1/Alb3 insertases: three independent gene duplications followed by functional specialization in bacteria, mitochondria and chloroplasts. Biol Chem. 2011;392(1-2):13-9.
48. Gaur R, Grasso D, Datta PP, Krishna PD, Das G, Spencer A, et al. A single mammalian mitochondrial translation initiation factor functionally replaces two bacterial factors. Mol Cell. 2008;29(2):180-90.
49. Brown A, Amunts A, Bai XC, Sugimoto Y, Edwards PC, Murshudov G, et al. Structure of the large ribosomal subunit from human mitochondria. Science 2014. 2014;346(6210):718-22.
50. Alberts B, Johnson A, Lewis J, Raff M, Roberts K, Peter Walter P. Molecular biology of the cell Fourth ed2002.
51. Schwartzbach CJ, Spremulli LL. Bovine mitochondrial protein synthesis elongation factors. Identification and initial characterization of an elongation factor Tu-elongation factor Ts complex. J Biol Chem 1989;264(32):19125-31.

52. Jeppesen MG, Navratil T, Spremulli LL, Nyborg J. Crystal structure of the bovine mitochondrial elongation factor Tu.Ts complex. J Biol Chem 2005;280(6):5071-81.
53. Eberly SL, Locklear V, Spremulli LL. Bovine mitochondrial ribosomes. Elongation factor specificity

J Biol Chem. 1985;260(15):8721-5.
54. Lee CC, Timms KM, Trotman CN, Tate WP. Isolation of a rat mitochondrial release factor. Accommodation of the changed genetic code for termination. J Biol Chem. 1987;262(8):3548-52.
55. Duarte I, Nabuurs SB, Magno R, Huynen M. Evolution and diversification of the organellar release factor family. Mol Biol Evol. 2012;29(11):3497-512.
56. Scolnick E, Tompkins R, Caskey T, Nirenberg M. Release factors differing in specificity for terminator codons. Proc Natl Acad Sci U S A. 1968;61(2):768-74.
57. sciences Trsao. Structure and function of the ribosome. Scientific background on the nobel prize in chemistry [Internet]. 2009:[2 p.]. Available from: https://www.nobelprize.org/nobel_prizes/chemistry/laureates/2009/advanced-chemistryprize2009.pdf.
58. Liu Q, Fredrick K. Intersubunit bridges of the bacterial ribosome. J Mol Biol. 2016;428(10 Pt B):2146-64.
59. Van der Sluis EO, Bauerschmitt H, Becker T, Mielke T, Frauenfeld J, Berninghausen O, et al. Parallel structural evolution of mitochondrial ribosomes and OXPHOS complexes. Genome Biol Evol. 2015;7(5):1235-51.
60. Sharma MR, Koc EC, Datta PP, Booth TM, Spremulli LL, Agrawal RK. Structure of the mammalian mitochondrial ribosome reveals an expanded functional role for its component proteins. Cell. 2003 115(1):97-108.
61. Greber BJ, Boehringer D, Leitner A, Bieri P, Voigts-Hoffmann F, Erzberger JP, et al. Architecture of the large subunit of the mammalian mitochondrial ribosome. Nature 2014;505(7484):515-9.
62. Yusupova G, Yusupov M. High-resolution structure of the eukaryotic 80S ribosome. Annu Rev Biochem. 2014;83:467-86.
63. Desmond E, Brochier-Armanet C, Forterre P, Gribaldo S. On the last common ancestor and early evolution of eukaryotes: reconstructing the history of mitochondrial ribosomes. Res Microbiol. 2011;162(1):53-70.
64. Amunts A, Brown A, Bai XC, Llácer JL, Hussain T, Emsley P, et al. Structure of the yeast mitochondrial large ribosomal subunit. Science. 2014;343(6178):1485-9.
65. Sharma MR, Booth TM, Simpson L, Maslov DA, Agrawal RK. Structure of a mitochondrial ribosome with minimal RNA. Proc Natl Acad Sci U S A. 2009;106(24):9637-42.
66. Zíková A, Panigrahi AK, Dalley RA, Acestor N, Anupama A, Ogata Y, et al. *Trypanosoma brucei* mitochondrial ribosomes: affinity purification and component identification by mass spectrometry. Mol Cell Proteomics. 2008;7(7):1286-96.
67. Ridlon L, Škodová I, Pan S, Lukeš J, Maslov DA. The importance of the 45 S ribosomal small subunit-related complex for mitochondrial translation in *Trypanosoma brucei*. J Biol Chem. 2013;288(46):32963-78.
68. Greber BJ, Boehringer D, Leibundgut M, Bieri P, Leitner A, Schmitz N, et al. The complete structure of the large subunit of the mammalian mitochondrial ribosome. Nature. 2014;515(7526):283-6.
69. Filipovska A, Rackham O. Pentatricopeptide repeats: modular blocks for building RNA-binding proteins. RNA Biol. 2013;10(9):1426-32.

70. Lightowlers RN, Chrzanowska-Lightowlers ZM. Human pentatricopeptide proteins: only a few and what do they do? RNA Biol. 2013;10(9):1433-8.
71. Montoya J, Ojala D, Attardi G. Distinctive features of the 5'-terminal sequences of the human mitochondrial mRNAs. Nature. 1981;290(5806):465-70.
72. Desai N, Brown A, Amunts A, Ramakrishnan V. The structure of the yeast mitochondrial ribosome. Science. 2017;355(6324):528-31.
73. Ott M, Prestele M, Bauerschmitt H, Funes S, Bonnefoy N, Herrmann JM. Mba1, a membrane-associated ribosome receptor in mitochondria. EMBO J 2006;25(8):1603-10.
74. Preuss M, Leonhard K, Hell K, Stuart RA, Neupert W, Herrmann JM. Mba1, a novel component of the mitochondrial protein export machinery of the yeast *Saccharomyces cerevisiae*. J Cell Biol. 2001 28(153):1085-96.
75. Maslov DA, Sharma MR, Butler E, Falick AM, Gingery M, Agrawal RK, et al. Isolation and characterization of mitochondrial ribosomes and ribosomal subunits from *Leishmania tarentolae*. Mol Biochem Parasitol. 2006;148(1):69-78.
76. Maslov DA, Spremulli LL, Sharma MR, Bhargava K, Grasso D, Falick AM, et al. Proteomics and electron microscopic characterization of the unusual mitochondrial ribosome-related 45S complex in *Leishmania tarentolae*. Mol Biochem Parasitol. 2007;152(2):203-12.
77. Suzuki T, Terasaki M, Takemoto-Hori C, Hanada T, Ueda T, Wada A, et al. Proteomic analysis of the mammalian mitochondrial ribosome. Identification of protein components in the 28 S small subunit. J Biol Chem. 2001;276(35):33181-95.
78. Suzuki T, Terasaki M, Takemoto-Hori C, Hanada T, Ueda T, Wada A, et al. Structural compensation for the deficit of rRNA with proteins in the mammalian mitochondrial ribosome. Systematic analysis of protein components of the large ribosomal subunit from mammalian mitochondria. J Biol Chem. 2001;276(24):21724-36.
79. Kitakawa M, Graack HR, Grohmann L, Goldschmidt-Reisin S, Herfurth E, Wittmann-Liebold B, et al. Identification and characterization of the genes for mitochondrial ribosomal proteins of *Saccharomyces cerevisiae*. Eur J Biochem. 1997;245(2):449-56.
80. De la Cruz VF, Lake JA, Simpson AM, Simpson L. A minimal ribosomal RNA: sequence and secondary structure of the 9S kinetoplast ribosomal RNA from *Leishmania tarentolae*. Proc Natl Acad Sci U S A 1985;82(5):1401-5.
81. Pusnik M, Small I, Read LK, Fabbro T, Schneider A. Pentatricopeptide repeat proteins in *Trypanosoma brucei* function in mitochondrial ribosomes. Mol Cell Biol. 2007;27:6876–88.
82. Lambert JD, Moran NA. Deleterious mutations destabilize ribosomal RNA in endosymbiotic bacteria. Proc Natl Acad Sci U S A. 1998;95(8):4458–62.
83. Neiman M, Taylor DR. The causes of mutation accumulation in mitochondrial genomes. Proc Biol Sci. 2009;726(1660):1201-9.
84. Lang BF, Burger G, O'Kelly CJ, Cedergren R, Golding GB, Lemieux C, et al. An ancestral mitochondrial DNA resembling a eubacterial genome in miniature. Nature. 1997;387(6632):493-7.
85. Lara E, Chatzinotas A, Simpson AG. *Andalucia* (n. gen.)--the deepest branch within jakobids (Jakobida; Excavata), based on morphological and molecular study of a new flagellate from soil. J Eukaryot Microbiol. 2006;53(2):112-20.
86. Flavin M, Nerad TA. *Reclinomonas americana* N. G., N. Sp., a new freshwater heterotrophic flagellate. J Eukaryot Microbiol. 1993;40(2):172-9.
87. O'Kelly CJ. The jakobid flagellates: structural features of Jakoba, Reclinomonas and Histiona and implications for the early diversification of eukaryotes. J Eukaryot Microbiol. 1993;40:627-36.

88. Pánek T, Táborský P, Pachiadaki MG, Hroudová M, Vlček Č, Edgcomb VP, et al. Combined culture-based and culture-independent approaches provide insights into diversity of jakobids, an extremely plesiomorphic eukaryotic lineage. Front Microbiol. 2015 6:1288.
89. Strassert JF, Tikhonenkov DV, Pombert JF, Kolisko M, Tai V, Mylnikov AP, et al. *Moramonas marocensis* gen. nov., sp. nov.: a jakobid flagellate isolated from desert soil with a bacteria-like, but bloated mitochondrial genome. Open Biol. 2016;6(2):150239.
90. Patterson DJ. *Jakoba libera* (Ruinen, 1938), a heterotrophic flagellate from deep oceanic sediments. Journal of the Marine Biological Association of the United Kingdom. 1990;70(2):381-93.
91. Rees T, Bailly N, Palomares D, Brands S, Gordon D, Robertson D, et al. Interim register of marine and nonmarine genera (IRMNG). In: (VLIZ) TFMI, editor. 2011.
92. Guiry MD, Guiry GM. AlgaeBase. In: World-wide electronic publication NUoI, Galway, editor. World register of marine species2018.
93. Vignais PV, Stevens BJ, Huet J, André J. Mitoribosomes from *Candida utilis*. Morphological, physical, and chemical characterization of the monomer form and of its subunits. J Cell Biol. 1972;54(3):468-92.
94. Rodríguez-Ezpeleta N, Teijeiro S, Forget L, Burger G, Lang BF. Construction of cDNA libraries: focus on protists and fungi. Methods Mol Biol. 2009;533:33-47.
95. Mansour FH, Pestov DG. Separation of long RNA by agarose-formaldehyde gel electrophoresis. Anal Biochem. 2013;441(1):18-20.
96. Tyanova S, Temu T, Cox J. The MaxQuant computational platform for mass spectrometry-based shotgun proteomics. Nat Protoc. 2016;11(12):2301-19.
97. Khusainov I, Vicens Q, Bochler A, Grosse F, Myasnikov A, Ménétret JF, et al. Structure of the 70S ribosome from human pathogen *Staphylococcus aureus*. Nucleic Acids Res 2016;44(21):10491-504.
98. De Silva D, Tu YT, Amunts A, Fontanesi F, Barrientos A. Mitochondrial ribosome assembly in health and disease. Cell Cycle. 2015;14(14):2226-50.
99. Bonen L, Calixte S. Comparative analysis of bacterial-origin genes for plant mitochondrial ribosomal proteins. Mol Biol Evol. 2006;23(3):701-12.
100. Sormani R, Masclaux-Daubresse C, Daniel-Vedele F, Chardon F. Transcriptional regulation of ribosome components are determined by stress according to cellular compartments in *Arabidopsis thaliana*. PLoS One. 2011;6(12):e28070.
101. Henderson R, Baldwin JM, Ceska TA, Zemlin F, Beckmann E, Downing KH. Model for the structure of bacteriorhodopsin based on high-resolution electron cryo-microscopy. J Mol Biol. 1990;213(4):899-929.
102. Petrossian TC, Clarke SG. Multiple motif scanning to identify methyltransferases from the yeast proteome. Mol Cell Proteomics. 2009;8(7):1516-26.
103. Szczepińska T, Kutner J, Kopczyński M, Pawłowski K, Dziembowski A, Kudlicki A, et al. Probabilistic approach to predicting substrate specificity of methyltransferases. PLoS Comput Biol. 2014;10(3):e1003514.
104. Park Y, Bader JS. How networks change with time. Bioinformatics. 2012;28(12):40-8.
105. Berman HM, Battistuz T, Bhat TN, Bluhm WF, Bourne PE, Burkhardt K, et al. The protein data bank. Acta Crystallogr D Biol Crystallogr. 2002;58(1):899-907.
106. Eddy SR. Profile hidden Markov models. Bioinformatics. 1998;14(9):755-63.
107. Claros MG, Vincens P. Computational method to predict mitochondrially imported proteins and their targeting sequences. Eur J Biochem. 1996;241(3):779-86.

108. Stojanovski D, Ryan MT, Wojtkowska M, Kmita H. Mitochondria protein import: methods. In: eLS [Internet]. 2017. Available from: http://www.els.net/WileyCDA/ElsArticle/refId-a0002617.html.

8. APPENDICES

8.1 Materials

Yeast Extract

Bacto Tryptone

NaCl

NaOH

AGAR

Glycerol 50 %

H_2O

$CuSO_4X5H_2O$

$ZnSO_4X7H_2O$

$CoCl_2X6H_2O$

$MnCl_2X4H_2O$

$NaMoO_4X2H_2O$

Biotin

B12

Thiamine HCL

HEPES

$CaCl_2X2H_2O$

$MgSO_4X7H_2O$

DMSO

Liquid nitrogen

SDS

Ice

DEPC-treated H_2O

Sucrose

Tris-HCL

$MgCl_2$

Tris

DTT

EDTA

SUPERase·In™

EDTA-free protease inhibitor

Trizol

Chloroform

Ambion glycogen

Isopropanol

70 % ethanol

Agarose

Ethidium bromide

Thermo Scientific RNA Gel Loading Dye (2X)

Boric acid

Acrylimide

TEMED

Ammonium persulfate (APS)

Glycine

Methanol

Acetic acid

Coomassie Brilliant Blue G-250

Milli-Q H_2O

Avian myeloblastosis virus (AMV) reverse transcriptase

Avian myeloblastosis virus (AMV) reverse transcriptase 5X buffer

dNTPs

Q5® High-Fidelity DNA Polymerase set

Formamide

Tricine

Triethanolamine

Formamide

Formaldehyde

Bromophenol blue

Na_3-citrate

NH_4Cl

8.2 Solutions and buffers

8.2.1 Solid LB

Component	Composition in 200 ml
Bacto™ Tryptone	2 g
Yeast extract	1 g
NaCl	10 g
1N NaOH	3 ml
Agar	3 g
50 % Glycerol	4.5 ml

Adjust pH to 7.5 with 1N NaOH. Complete the volume to 200 ml and autoclave.

8.2.2 Liquid LB

Component	Composition in 200 ml
Bacto™ Tryptone	2 g
Yeast extract	1 g
NaCl	10 g
1N NaOH	3 ml

Adjust pH to 7.5 with 1N NaOH. Complete the volume to 200 ml and autoclave.

8.2.3 Trace elements

Stock solution	Volume added in a final 1 L medium	Final concentration
CuSO4X5H₂O (0.98 g/100 ml)	1 ml	0.0098 mg/L
ZnSO4X7H₂O (2.20 g/100 ml)	1 ml	0.0220 mg/L
CoCl2X6H₂O (1.0 g/100 ml)	1 ml	0.0100 mg/L
MnCl2X4H₂O (1.8 g/100 ml)	1 ml	0.0180 mg/L
NaMoO4X2H₂O (0.63 g/100 ml)	1 ml	0.0063 mg/L

Complete the volume to 1 L and autoclave.

8.2.4 1000X Vitamins

Component	Composition in 100 ml	Final concentration
Biotin	0.1 mg	0.001 mg/L
B12	1.1 mg	0.011 mg/L
Thiamine HCL	20 mg	0.200 mg/L

Complete the volume to 100 ml. Filter in a 0.22 μm membrane.

8.2.5 1000X Trace elements

Component	Final concentration
$NaNO_3$	75 g/L
$NaHCO_3$	12.6 g/L
H_3BO_3	6 g/L
KCL	7.45 g/L
$NaH_2PO_4XH_20$	5 g/L
NH_4Cl	2.65 g/L

8.2.6 WCL medium for protists

Component	Volume added in 1 L	Final concentration
1M HEPES pH 7.5	10 ml	10 mM
$CaCl_2X2H_2O$ (36.76 g/L)	1 ml	36.6 mg/L
$MgSO_4X7H_2O$ (36.97 g/L)	1 ml	36.97 mg/L
1000X Trace elements	1 ml	1X
1000X Vitamins	1 ml	1X

Complete the volume to 1 L with previously autoclaved distilled H_2O.

8.2.7 40% (w/w) sucrose gradient buffer

Component	Composition for one sample	Final concentration
50% Sucrose	3.2 ml	40 %
1M Tris-HCL	20 µL	5 mM
1M $MgCl_2$	4 µL	1 mM
1M DTT	4 µL	1 mM
0.5 M EDTA	1 µL	0.125 mM
DEPC-treated H_2O	0.771 ml	-

8.2.8 15% (w/w) sucrose gradient buffer

Component	Composition for one sample	Final concentration
50% Sucrose	0.72 ml	15 %
1M Tris-HCL	12 µL	5 mM
1M $MgCl_2$	2.4 µL	1 mM
1M DTT	2.4 µL	1 mM
0.5 M EDTA	0.6 µL	0.125 mM
DEPC-treated H_2O	1.6626 ml	-

8.2.9 Homogenization buffer A

Component
5 mM Tris-HCL
1 mM $MgCl_2$
1 mM DTT
0.25 mM EDTA

8.2.10 Homogenization buffer B

Component
10 mM Tris-HCL
10 mM $MgCl_2$
1mM DTT
1 mM EDTA

8.2.11 Homogenization buffer C

Component
100 mM Tris-HCL
5 mM $MgCl_2$
50 mM NH_4Cl
1 mM DTT

8.2.12 Homogenization buffer D

Component
20 mM Tris-HCL
10 mM $MgCl_2$
30 mM NH_4Cl
1 mM DTT

8.2.13 Lysis buffer A

Component
5 mM Tris-HCL
1 mM $MgCl_2$
1 mM DTT
0.25 mM EDTA
2% Triton

8.2.14 Lysis buffer B

Component
10 mM Tris-HCL
10 mM $MgCl_2$
1mM DTT
1 mM EDTA
2% Triton

8.2.15 Lysis buffer C

Component
100 mM Tris-HCL
5 mM $MgCl_2$
50 mM NH_4Cl
1 mM DTT
2% Triton

8.2.16 Lysis buffer D

Component
20 mM Tris-HCL
10 mM $MgCl_2$
30 mM NH_4Cl
1 mM DTT
2% Triton

8.2.17 5X TBE

Component	Composition in 4 L	Final concentration
EDTA 0.5 M	80 ml	0.01 mM
Boric acid powder	110 g	27.5 g/L
Tris powder	216 g	54 g/L

Complete volume to 4 L.

8.2.18 50X TT

Component	Composition in 4 L	Final concentration
99% Tricine	31.93 g	7.98 g/L
99% Triethanolamine	26.6 ml	6.58%

Complete volume to 4 L.

8.2.19 1 % Agarose gel

Component	Composition in 70 ml	Final concentration
Agarose	0.7 g	0.01 g/ml
Ethidium bromide (10 mg/ml)	1.75 µl	0.25 mg/ml

Complete volume to 70 ml with 0.5 X TBE.

8.2.20 2 % Agarose gel

Component	Composition in 70 ml	Final concentration
Agarose	1.4 g	0.02 g/ml
Ethidium bromide (10 mg/ml)	1.75 µl	0.25 mg/ml

Complete volume to 70 ml with 0.5 X TBE.

8.2.21 2% Agarose gel with Formaldehyde

Component	Composition in 100 ml	Final concentration
Agarose	2 g	0.02 g/ml
37 % Formaldehyde	3 ml	1.11 %
50X TT	2 ml	1X

Complete the volume 100 ml with distilled H_2O.

8.2.22 SDS-PAGE gel

- 4 % Stacking gel

Component	Composition in 5 ml	Final concentration
49.5 % Acrylimide	0.39 ml	3.82 %
Tris-HCL 1M pH 6.8	0.625 ml	123.64 mM
10% SDS	50 µL	0.1 %
TEMED	5 µL	0.01%
10% Ammonium persulfate (APS)	50 µL	0.1 %
H_2O	3.935 ml	-

- 18 % Separation gel

Component	Composition in 10 ml	Final concentration
49.5 % Acrylimide	3.564 ml	17.64 %
Tris-HCL 1M pH 6.8	2.5 ml	250 mM
10% SDS	100 µL	0.1 %
TEMED	10 µL	0.1 %
10% Ammonium persulfate (APS)	32 µL	0.32 %
H_2O	3.794 ml	-

8.2.23 5X SDS-PAGE loading buffer

Composition
0.313 M Tris pH 6.8
10 % SDS
0.05% BPB
0.65M DTT
50% Glycerol

8.2.24 5X Tris-Glycine SDS-PAGE running buffer

Component	Composition in 1 L	Final concentration
125 mM Tris pH 8.3	125 mL	15.63 mM
760 mM glycine	72.06 g	69.18 mM
0.5 % SDS	50 mL	0.025 %

Complete volume to 1 L.

8.2.25 Protein fixation solution

Composition
50 % Methanol
7 % acetic acid

8.2.26 Distaining solution

Composition
10 % Methanol
7 % acetic acid

8.2.27 20X SSC

Composition in 1 L	Final concentration
175.3 g NaCl	3M
88.2 g Na3-citrate	342 mM
800 ml H_2O	-

Adjust pH to 7.0 and volume to 1 L. Then, autoclave it.

8.2.28 UA buffer

Composition
8M urea
0.1M Tris-HCl pH 8.5

8.3 Primers used in RT-PCR

- ag01 (mt-LSU-rRNA, forward):
  TCTAATGGGAATTTGACGAACAC
- ag02 (mt-LSU-rRNA, reverse; 23S bt-rRNA, reverse):
  TCGCTACCTTAGGACCGTTA
- ag05 (mt-SSU-rRNA, forward):
  AGAAGGGTGATGGTTTGACAGG
- ag06 (mt-SSU-rRNA, reverse; 16S bt-rRNA, reverse):
  TGGTGTGACGGGCGGTGT
- eb01 23S (23S bt-rRNA, forward):
  CTGAGGTGTGATGACGAGGC
- eb04 (16S bt-rRNA, forward):
  CCTTCGGGAACTCTGAGACAG
- NS5fwd (cyt-SSU-rRNA, forward):
  GACGGAAGGGCACCACC
- BMB-C-rev (cyt-SSU-rRNA, reverse):
  CGACGGGCGGTGTGTAC

8.4 Probes used in Northern blot

- ag03: (12S mt-SSU-rRNA):
  TGTCAAACCATCACCCTTCTTCTCTCAAA
- ag04 (mt-LSU-rRNA):
  CCCAATTCTGTGCCGCCTATGAAACA
- eb02 (16S bt-rRNA):
  GTCTCAGAGTTCCCGAAGGCACCAA
- eb03: (23S bt-rRNA):
  TGCCTCGTCATCACACCTCAGCGT